MICROCOPY RESOLUTION TEST CHART

NATIONAL BUREAU OF STANDARDS-1963-A

DRES

SUFFIELD TECHNICAL PAPER

NO. 449

BLAST RESPONSE OF UHF POLEMAST ANTENNA
- EVENT DICE THROW (U)

by

C.G. Coffey and G.V. Price

D D C
FEB 2 1978
RECEIVED
F

PROJECT NO. 97-80-01

November 1977

DEFENCE RESEARCH ESTABLISHMENT SUFFIELD : RALSTON : ALBERTA

REPORT NO: SUFFIELD TECHNICAL PAPER NO. 449

PROJECT NO: 97-80-01

TITLE: Blast response of UHF polemast antenna
                              - event dice throw (U)

DATED: November 1977

AUTHORS: C.G. Coffey & G.V. Price

SECURITY GRADING: UNCLASSIFIED Initial distribution January 1978

UNCLASSIFIED

UNLIMITED
DISTRIBUTION

DEFENCE RESEARCH ESTABLISHMENT SUFFIELD
RALSTON   ALBERTA

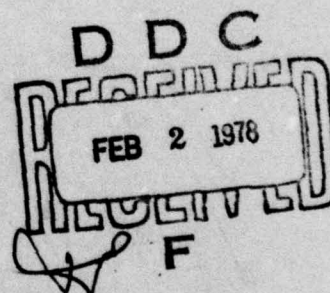SUFFIELD TECHNICAL PAPER NO. 449

BLAST RESPONSE OF UHF POLEMAST ANTENNA
- EVENT DICE THROW (U)

by

C.G. Coffey and G.V. Price

PROJECT NO. 97-80-01

UNCLASSIFIED

ACKNOWLEDGEMENT

DEFENCE RESEARCH ESTABLISHMENT SUFFIELD
RALSTON ALBERTA

SUFFIELD TECHNICAL PAPER NO. 449

BLAST RESPONSE OF UHF POLEMAST ANTENNA
- EVENT DICE THROW (U)

by

C.G. Coffey and G.V. Price

ABSTRACT

The blast response of a 23 ft UHF Polemast Antenna was investigated
in a free-field blast trial and in numerical simulation experiments.
The antenna satisfactorily withstood the air blast loading at the nominal
7.0 psi peak overpressure location in Event Dice Throw, and the numerical
model predictions for the natural frequencies and transient strain were
in excellent agreement with the values obtained experimentally.

(U)

DEFENCE RESEARCH ESTABLISHMENT SUFFIELD
RALSTON ALBERTA

SUFFIELD TECHNICAL PAPER NO. 449

BLAST RESPONSE OF UHF POLEMAST ANTENNA
- EVENT DICE THROW (U)

by

C.G. Coffey and G.V. Price

INTRODUCTION

The Defence Research Establishment Suffield (DRES), in support
of the Canadian Forces (Maritime) policy on blast hardening of ships and
sub-components, has conducted a series of tests to determine the ability
of certain antenna designs to withstand blast overpressures of various
intensities. During Event Dice Throw, a 620 ton AN/FO free-field blast
trial conducted by the United States Defence Nuclear Agency at the White
Sands Missile Range in New Mexico on 6 October, 1976, several antenna
designs were tested at various overpressure levels. One of the antennas
evaluated in the trial was a 23 ft UHF Polemast Antenna, of the type
intended for several classes of ships (IRE-257, DDE-261, DDH-265, and
AOR508).

The objectives of this study were to determine the ability of
the Polemast Antenna Assembly, complete with attached fibreglass covered
radiators, to withstand a blast wave at the 7.0 psi peak overpressure
level, and to compare the measured antenna response against theoretical
predictions determined by a computer model recently developed at DRES
[1]. It is intended that experimental verification of the computer
model would lead to a criterion for predicting the blast response of
polemast designs in general.

CONSTRUCTION OF THE PROTOTYPE POLEMAST ANTENNA

A prototype Polemast Antenna was constructed at DRES in accordance with drawings supplied by DMCS-6. During the fabrication of the prototype, design modifications were required in order to accommodate the facilities of the DRES Machine Shop. The design modifications are examined in detail in Appendix A. It is anticipated that the suggested design changes will generally make the antenna more cost effective by simplifying the fabrication procedures.

A schematic view of the Polemast Antenna is shown in Figure 1. The structural portion of the antenna is a seamless aluminum tube 9.5" O.D. x 0.261 " wall x 19'-7" long. The tubing was fabricated by Alcan Canada Products Ltd., and a summary of the physical properties of the tubing is provided in Appendix B. Attached to the aluminum tubing were an Upper and Lower Radiator, a Lower Transformer, a Cross Arm, and an AN/SRD-501 Antenna at the mast head. The Lower Radiator and Transformer were actual test items, while the Upper Radiator and the AN/SRD-501 Antenna were mock-ups constructed to simulate the approximate weight and projected cross-sectional area of the respective items.

The Prototype Polemast Antenna was mounted vertically in a lattice structure at the nominal 7.0 psi peak overpressure level, 1135 ft from ground zero (GZ). The lattice structure was used in a previous multi-ton trial ("Event Dial Pack" held at DRES in 1970) as a mounting for a GRP Topmast [2]. The lattice structure and mountings for the Polemast are shown in Figure 2. As shown in the figure, the distance between the clamp assemblies attaching the Polemast to the lattice structure was 36 in. The upper clamp assembly was in accordance with drawing DDDS-000143 supplied by DMCS-6 (a change in this design is recommended, as noted in Appendix A). The lower clamp assembly, as shown in Figure 2, was different from that specified in drawing DDDS-000157 supplied by DMCS-6. Changes to this assembly were introduced to expedite assembly in the field (see Figure 2, Section B-B). The modifications to the lower clamp assembly did not in any way affect the structural integrity of the joint.

The lattice structure was mounted on a 12 ft x 6 ft x 2.5 ft

heavy reinforced concrete foundation (DRES drawing MES-CDT-100-C2-1).
The Polemast and Antenna components were assembled while lying horizontal,
and the complete assembly was lifted with a crane over the lattice
structure and lowered into place. After the upper and lower clamp
assemblies were secured, no further adjustments were required since the
upper and lower mounting plates on the lattice structure were normal to
the uprights and parallel to the level of the concrete pad. The complete
Polemast assembly (excluding the lattice structure) weighed approximately
348 pounds. .This may be compared to the weight of the corresponding
Polemast Antenna for ship use, estimated at 463 pounds. The difference
in weight is due to the weight of additional clamps and cables used
aboard ship which were considered unnecessary for the blast trial.

A photograph of the completed prototype Polemast Antenna
installed for the Event Dice Throw field trial is shown in Figure 3.
The orientation of the Polemast with respect to the direction of the
blast is shown in Figure 1. As indicated in the figure, the fore-aft
line of the Polemast was oriented   normal to the direction of the
blast, thereby resulting in the maximum blast loading on the brackets
supporting the Radiators.

INSTRUMENTATION

Five pairs of MICRO-MEASUREMENTS type CEA-13-250UW-120 strain
gauges were bonded directly to the aluminum tubing of the prototype
Polemast. The strain gauge locations are shown in Figure 1. The gauges
which constitute a strain gauge pair were bonded to opposite sides of
the aluminum tubing on a line corresponding to the blast direction,
thereby measuring the maximum flexural strain at the specified cross-
sections. The signals from the strain gauge pairs were conditioned with
bridge and balance units, amplified, F.M. multiplexed and then recorded
on 14 track magnetic tape with a frequency response of DC to 4 KHz. In
this fashion, five channels of experimental data were multiplexed onto
one tape channel, a procedure which was required by the large number of
DRES data channels and limited number of tape recorders. A block diagram
describing the instrumentation is shown in Figure 4, and a photograph of
the DRES Instrumentation Bunker in which the data signals were processed

and recorded is shown in Figure 5.

In addition to the strain gauge data, the response of the prototype Polemast was recorded on a LOCAM high-speed camera pre-set to run at 500 frames per second. Confirmation of the camera speed was arranged through the use of a time mark generator.

COMPUTER MODEL SIMULATION

A numerical procedure was developed at DRES to predict the elastic response of a variable cross-section cantilever beam when subjected to a transient air blast load [1]. The procedure begins with the Bernoulli-Euler equation of a vibrating beam. The normal modes and natural frequencies of the beam are determined by solving the differential equations for free vibration using successive relaxation, Rayleigh quotient and Gram-Schmidt orthogonalization numerical techniques. The forced vibration solution is obtained using normal mode coordinates and Laplace transforms.

The computer model simulation used in pin-pin-free boundary condition of the form

(1) <u>pin</u> at x=0, zero displacement and moment,

(2) <u>pin</u> at x=3 ft, zero displacement,

(3) <u>free</u> at x=L, zero moment and shear,   (1)

where x is a distance coordinate measured from the base of the antenna, and L is the length of the antenna. In addition, the following values for the drag coefficient C_D were used in computing the aerodynamic drag portion of the blast wave loading on the antenna: [3, 4].

$$C_D = \left\{ \begin{array}{ll} 0.7 \ , & M \geq 0.48, \ Re \geq 3 \times 10^5, \\ 0.6 \ , & M < 0.48, \ Re \geq 3 \times 10^5, \\ 1.2 \ , & M < 0.48, \ Re < 3 \times 10^5. \end{array} \right\} \quad (2)$$

In the above equation, M is the instantaneous Mach number of the flow incident on the antenna, and Re is the instantaneous Reynolds number (based on local diameter).

The structure of the Polemast Antenna was represented in the

computer model in such a way as to simulate the mass and projected
(normal to blast direction) cross-sectional area profiles of the prototype.
The physical features which describe the prototype Antenna and the
corresponding computer simulation of the antenna are respectively outlined
in Tables 1 and 2. It should be noted that the computer simulation of
the antenna agrees with the actual structure of the prototype in the
following critical areas: weight distribution, total weight, projected
(normal to blast direction) cross-sectional area distribution, and total
projected cross-sectional area.

COMPARISON OF THEORETICAL AND EXPERIMENTAL NATURAL FREQUENCIES

TWANG TEST

Prior to the blast trial, a "Twang Test" was performed to obtain
free vibration strain data for the prototype Polemast. A static load was ap-
applied near the top of the antenna using an anchored wire rope at a pull
angle of 30° to the horizontal. The load was subsequently released suddenly
with the aid of an electrical solenoid and the strain data for free vibration
were recorded. The experiment was performed to determine the natural frequencies
of the antenna and to verify the test instrumentation.

A photograph of the Twang Test apparatus is shown in Figure 6.
The apparatus consisted of a 1/4 in wire rope attached to a bracket at
the top of the Polemast and anchored to a truck, a 6000 lb capacity
L.A.B. Corp. Quick Release Hook, a hand-operated mechanical winch to
take up slack in the system, a hydraulic (pull) cylinder for fine load
adjustments, and a Transducers Inc. strain-type load cell (model ML2-
151-1K) with a Budd strain indicator readout (model P-350) to measure
the applied load. The applied load was monitored locally with the load
cell while the bending strains as measured by the strain gauges bonded
to the antenna were recorded remotely in the Instrumentation Bunker.

A comparison of predicted and measured peak bending strains
(prior to the electric release of the load on the antenna) is presented
in Table 3. The predicted strains were found to be in good agreement
with the values obtained experimentally.

The load on the antenna was released electrically and the
bending strain data for free vibration were recorded in the Instrumentation
Bunker. In this fashion it was possible to establish that the field
instrumentation was operational.

A Fourier analysis was subsequently performed for the experimental
strain data to determine the natural frequencies of the antenna. The
free vibration strain history and corresponding Fourier analysis for
gauges 3 and 5 are presented in Figures 7 and 8. The lowest natural
frequency is sharply identified as 4.00 cps by the Fourier analysis,
while the higher natural frequencies are less distinct or not apparent.
The best resolution of the higher natural frequencies occurs for the
gauge located closest to the centre of the antenna, gauge 5, and only a
weak band of indistinct higher frequencies in the range 19.7 to 32.1 cps
is apparent.

The theoretical (numerical simulation) predictions for the
three lowest natural frequencies and corresponding normal modes are
presented in Figure 9, and a comparison of theoretical and experimental
natural frequencies is presented in Table 4. It is apparent from this
comparison that the predicted frequencies are in good agreement with the
values obtained experimentally.

COMPARISON OF THEORETICAL AND EXPERIMENTAL BENDING STRAIN HISTORIES

EVENT DICE THROW

The theoretical (numerical simulation) model was used to
generate two sets of bending strain predictions. The first predictions
(set A) were produced using a Friedlander overpressure wave which corresponds
to the nominal Defense Nuclear Agency (DNA) pre-trial predictions for
peak overpressure (7.0 psi), positive duration (242 msec) and positive
phase impulse (600 psi-msec). The second predictions (set B) were
produced using a Friedlander overpressure wave which corresponds to the
average measured[1] peak overpressure (6.6 psi), positive duration (251

---

[1] The free-field overpressure at the base of the antenna was measured using
four Bytrex Model HFH-100 strain-type pressure transducers [5]. The
"measured" overpressure wave properties were considered to be the average
of the properties determined by the individual pressure transducers.

msec) and positive phase impulse (705 psi-msec) of the blast wave itself.

A comparison of the above two overpressure waves is presented in Table 5 and Figure 10. It should be noted that despite the lower peak overpressure in the experimental Friedlander wave, the total impulse associated with the experimental wave is approximately 18% higher than the corresponding impulse of the predicted wave.

A comparison of theoretical (numerical simulation) and experimental (blast trial) strain histories for the two sets (A and B) of bending strain predictions is presented in Figures 11 and 12. The comparison for prediction set B is repeated in Figures 13 to 17 in an enlarged format; in general, the predicted strains are found to be in excellent agreement with the experimental strains.

The strain predictions B are somewhat larger than predictions A, a result due to the larger positive phase impulse over the first quarter period (63 msec) in B compared to A.

The very small bending strains measured by gauge 1 and the corresponding small predicted strain at this location provided experimental verification of the assumed "pin" boundary condition (zero displacement and moment) at the base of the simulated antenna.

As expected, the largest predicted and measured strains occur at gauge 3, located slightly above the upper clamp assembly.

Finally, it is noted that the predicted strains for gauge 5 display excessively strong contributions from the second natural frequency (25.5 cps) and normal mode compared to the measured strain history at this location. Although the measured strain history at this location begins with a superimposed strain component corresponding to the second natural frequency, the superimposed component rapidly diminishes with time, demonstrating strong selective damping of the second mode compared to the fundamental mode. Since the numerical simulation model has no provisions for damping, the second mode in the strain predictions does not diminish with time. This accounts for the observed differences between the predicted and measured strains at gauge 5. The differences would be reduced significantly if the numerical simulation model was extended to include the effects of damping.

A general evaluation of the ability of the numerical simulation model to predict peak bending strains is presented in Table 6. It is apparent from this table that there is excellent agreement between predicted and experimental peak bending strains, since the average ratio of peak theoretical to experimental bending strain from all five gauge pairs is 1.19 for predictions A and 1.25 for predictions B.

SUPPLEMENTAL EXPERIMENTS

SIMPLIFIED ANTENNA SIMULATION

A third set of strain predictions (set C) was produced to determine the effect of the mass of the antenna assemblies (Lower and Upper Radiator, SRD-501 Antenna) on the transient response of the Polemast in general. The structure of the simulated antenna in this case was assumed to be the same as the structure described in Table 2, with the exception of the interior diameter profile (ID) which was changed to 8.978 in at all positions along the antenna. This change was equivalent to neglecting the mass of the antenna assemblies and including only the uniform mass distribution of the aluminum tubing. In all other regards, this simulation experiment was identical to the previous prediction experiment A.

A comparison of strain prediction set C against the measured natural frequencies and bending strains is presented in Figure 18 and Table 7. It is apparent from this comparison that the natural frequencies and bending strains C are considerably poorer than the corresponding predictions A which were obtained using a more realistic simulated mass profile. This demonstrates the critical importance of having the computer mass profile simulation agree with the actual structure of the antenna.

VOLTAGE STANDING WAVE RATIO TEST

Tests were performed before and after the blast trial to determine the effect of the blast wave on the Voltage Standing Wave Ratio (VSWR) of the fibreglass covered Radiator. Only the Lower Radiator was evaluated, since the Upper Radiator was a mock-up unit. The pre-

trial and post-trial VSWR tests were conducted by the DMCS-6 Project
Officer on 30 September and 6 October, 1976 [6]. Additional information
relating to the VSWR measurement techniques and equipment may be obtained
from the DMCS-6 Project Officer.

The pre-shot and post-shot VSWR test results are shown in
Figure 19. Calculations for the VSWR versus frequency are shown in
Figure 20. It should be noted that the pre-shot VSWR test was performed
without the Screen (Drawing Number 000-000145) while the post-shot test
was performed with the Screen in place. However, the presence or absence
of the Screen was found to have no influence on the VSWR test, since a
further post-shot VSWR test without the Screen produced results imperceptibly
different from the post-shot VSWR test with the Screen in place.

It is apparent from the VSWR measurements and comparisons in
Figures 19 and 20 that the blast wave caused no immediate deterioration
in the electrical performance of the Lower Radiator. In addition, a
visual inspection of the Lower Radiator indicated no evidence of physical
damage arising from the blast wave.

CROSS-ARM DEFLECTION TEST

At the request of the Polemast design authority, a simple
bending test was conducted on the Cross-Arm Assembly (Drawing DDDS-
000146) located at the Mast Head. The test was performed to determine
the load versus deflection on one of the four arms, the yield point of
the arm, and the corresponding arm safety factor.

The apparatus consisted of a 1/2 in wire rope attached to one
of the four arms (the attachment point was a hole in the web on the arm,
16 in from the mast centreline) and anchored to a bolt in the concrete
base (loading was normal to the arm), a turnbuckle to apply the load,
and a Transducer Inc. strain-type load cell (model BTC-FM52-CD-10K) with
a Budd strain indicator readout (model P-350) to measure the applied
load.

The results from this test are presented in Table 8. In the
first loading application, the cross-arm demonstrated a linear load-
deflection behavior up to 3500 lb, and the arm retained a permanent

deflection of 1/4 in on release of the load. A similar linear relationship
(up to 3500 lb) was apparent in a second loading application, and increasing
the load to 6000 lb resulted in a permanent deflection of 7/8 in on
release of the load. No other deformation of the assembly was apparent.

It was concluded that the cross-arm yield point is in the
vicinity of 3000 lb (vertical load) and the arm is capable of withstanding
a vertical load of 6000 lb with only a small amount of permanent deformation.

CONCLUSIONS

The blast response of a 23 ft UHF Polemast Antenna was investigated
in a free-field blast trial and in numerical simulation experiments.
The Polemast Antenna, complete with fibreglass covered radiators, satisfactorily
withstood the air blast loading at the nominal 7.0 psi peak overpressure
location in Event Dice Throw. The corresponding antenna response was
modelled numerically, and the computed natural frequencies and transient
strains were in excellent agreement with the values obtained experimentally.
Subject to an accurate numerical simulation of the antenna's mass and
projected (normal to blast direction) cross-sectional area profiles, the
computer model is recommended as a design tool in the development of
polemast designs in general.

1 x (ft)	2 ID (in)	2 OD (in)	3 OD (in)	Weight (lb)
0	8.978	9.500	9.500	
				26.8
3	8.978	9.500	9.500	
				26.8
6	8.978	9.500	9.500	
				26.8+24.0[4]
9	8.978	9.500	22.81[4]	
				26.8+24.0[4]
12	8.978	9.500	9.500	
				26.8
15	8.978	9.500		
			22.81[5]	26.8+37.0[5]
18	8.978	9.500		
				13.4
21	SRD-501 Antenna (19.58 to 22.83 ft)	SRD-501 Antenna (19.58 to 22.83 ft)	25.75[6]	89.0[6]
				<u>348</u> Total

[1] Distance from the base of the antenna.

[2] This profile corresponds to the extruded aluminum tubing.

[3] This profile corresponds to the complete antenna (tubing plus antenna assemblies).

[4] Lower Radiator.

[5] Upper Radiator.

[6] SRD-501 Antenna.

$E = 10 \times 10^6$ psi

$\rho = 0.003044$ slugs/in^3

<u>TABLE 1</u>: Physical features of the prototype Polemast Antenna.

x (ft)[1]	ID (in)[2]	OD (in)[2]	OD (in)[3]	Weight (lb)
0[7]	8.978	9.500	9.500	
				26.8
3[7]	8.978	9.500	9.500	
				26.8
6	8.978	9.500	9.500	
				50.8[4]
9	7.950	9.500	17.22[4]	
				50.8[4]
12	8.978	9.500	9.500	
				35.9[5]
15	8.600	9.500	13.36[5]	
				45.1[5]
18	8.600	9.500	13.36[5]	
				52.4[6]
21	8.290	9.500	10.08[6]	
				59.6[6]
24[7]	8.290	9.500	10.08[6]	
				348 Total

[1] Distance from the base of the antenna.

[2] This profile is calculated to establish the correct mass distribution, assuming a fixed OD equal to that of the seamless extruded aluminum tubing which constitutes the primary structural portion of the antenna.

[3] This profile is calculated to establish the correct projected (normal to blast direction) cross-sectional area distribution.

[4] Includes a contribution from the Lower Radiator.

[5] Includes a contribution from the Upper Radiator.

[6] Includes a contribution from the SRD-501 Antenna.

[7] Boundary conditions: pin at x=0 ft, pin at x=3 ft, free at x=24 ft.

$E = 10 \times 10^6$ psi
$\rho = 0.003044$ slugs/in^3
$\Delta x = 3$ ft
$N = 8$
$L = 24$ ft

TABLE 2: Physical features of the computer simulation of the prototype Polemast Antenna. The calculated profiles in this table are dependent on the distance between data points (Δx).

Gauge	Bending Strain (µin/in)[1] Cable Load is 808 lb		
	Predicted	Measured[2]	Pred./Meas.
1	68	43	1.58
2	408	328	1.24
3	817	771	1.06
4	743	767	0.97
5	371	400	0.93
			Avg. 1.16

[1] The cable load of 808 lb was applied to the antenna at a pull angle of 30° to the horizontal. The corresponding horizontal component of the load was 700 lb. This loading was reached in three approximately equal stages. The horizontal deflection at the top of the mock-up SRD-501 Antenna corresponding to the 808 lb cable load was 3.5 in (measured using a transit, 5% reading uncertainty).

[2] The bending strains were recorded in the Instrumentation Bunker using the same procedures to be followed in the blast trial itself.

TABLE 3: Twang Test bending strains prior to the electric release of the load.

Mode	Natural Frequencies (cps)		
	Theoretical	Experimental	Theo./Exp.
1	4.62	4.00	1.16
2	25.5	24.1[1]	1.06
3	72.4	——	——

[1] This value represents an average of indistinct frequencies which appear in band over the range 19.7 to 32.1 cps.

TABLE 4: A comparison of theoretical (numerical simulation) and experimental (Twang Test) natural frequencies for the Polemast Antenna.

Symbol	Description	Set A	Set B
P_A (psi)	atmospheric pressure	12.58	12.42
T_A (°F)	atmospheric temperature	54.0	48.0
p_o (psi)	peak overpressure	7.0	6.6
t_d (msec)	positive phase duration	242	251
I_D (psi-msec)	positive phase impulse	600	705
κ (computed)[2]	Friedlander decay constant	1.127[2]	0.505[2]
Δt (msec)	time step in the numerical[1] integration	1.00	1.00

[1] The numerical simulation of the time response is formed using only the lowest 3 natural frequencies and corresponding normal modes.

[2] The decay constant is computed based on the condition that the Friedlander wave be characterized by the specified values of p_o, t_d and I_D.

TABLE 5: Air blast data used in the theoretical (numerical simulation) model to generate prediction sets A and B.

Gauge	Peak Bending Strains (µin/in)				
	Experimental	Predictions A		Predictions B	
		Theoretical	Theo./Exp.	Theoretical	Theo./Exp.
1	132	208	1.58	222	1.68
2	973	1248	1.28	1333	1.37
3	2010	2414	1.20	2582	1.28
4	1917	2008	1.05	2160	1.13
5	927	774	0.83	737	0.80
			Avg 1.19		Avg 1.25

TABLE 6: Comparison of peak theoretical and experimental bending strains (first quarter cycle only).

Mode	Natural Frequencies (cps)		
	Predictions C	Experimental [1]	Pred./Exp.
1	5.03	4.00	1.26
2	30.2	24.1	1.25
3	79.7	———	———

[1] Twang Test data reported in Table 4.

Gauge	Peak Bending Strain (μin/in)		
	Predictions C	Experimental [2]	Pred./Exp.
1	295	132	2.23
2	1769	973	1.82
3	3445	2010	1.71
4	2985	1917	1.56
5	1399	927	1.51
			Avg 1.77

[2] Blast trial data reported in Table 6.

TABLE 7: Comparison of strain prediction set C against the measured natural frequencies and bending strains.

First Loading		Second Loading	
Load[1] (lb)	Deflection[2] (in)	Load[1] (lb)	Deflection[2] (in)
100	0	100	0
1000	1/4	1000	1/4
2000	1/2	2000	1/2
3000	3/4	3000	3/4
4000	1-1/16	4000	7/8
		5000	1-5/16
		6000	1-5/8

[1] The load was measured by a load cell and is accurate to 0.1%.

[2] The deflection was measured by hanging a weight from the cross-arm and measuring the vertical displacement of the weight at ground level (measurement uncertainty is of the order of 1/16 in).

TABLE 8:   Cross-arm deflection test.
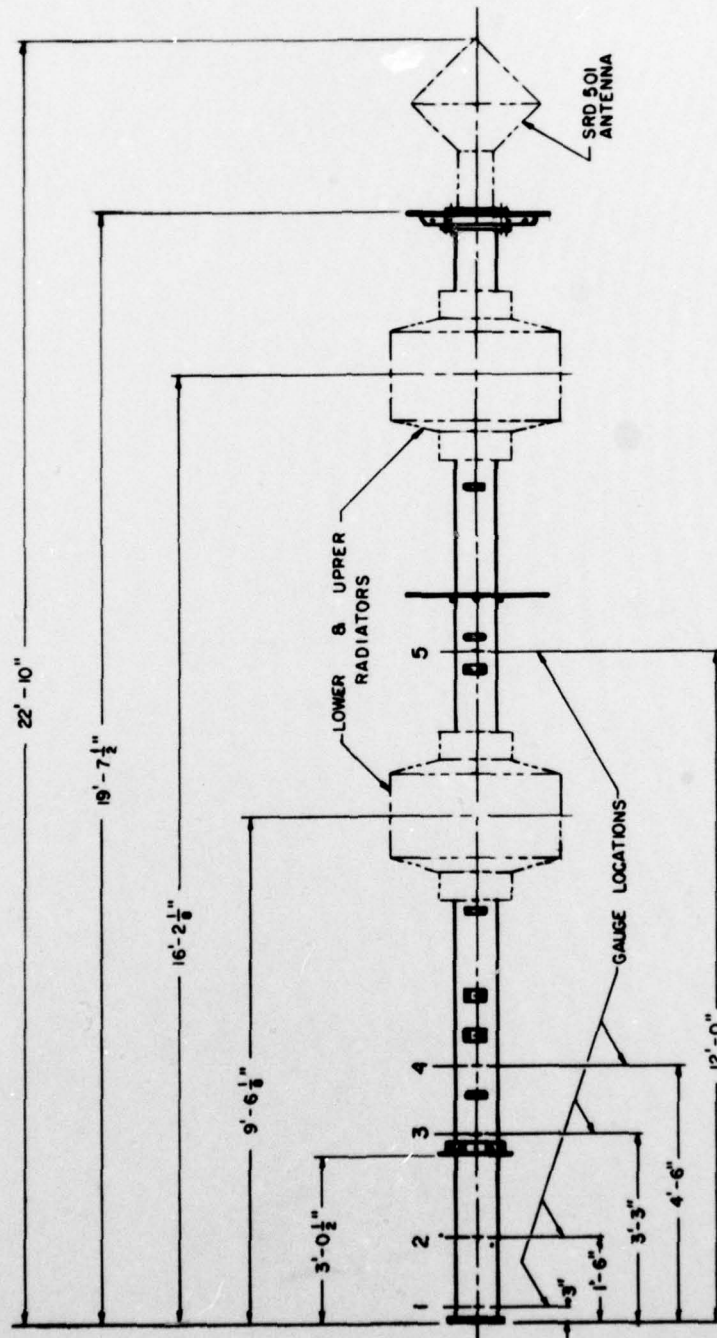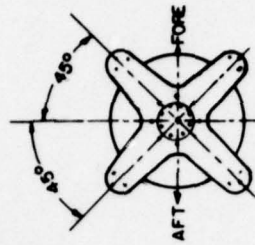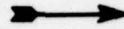
FIG. 1 SCHEMATIC OF THE PROTOTYPE POLEMAST ANTENNA, INCLUDING THE LOCATIONS OF THE
STRAIN GAUGES

SECTION B-B

SECTION A-A
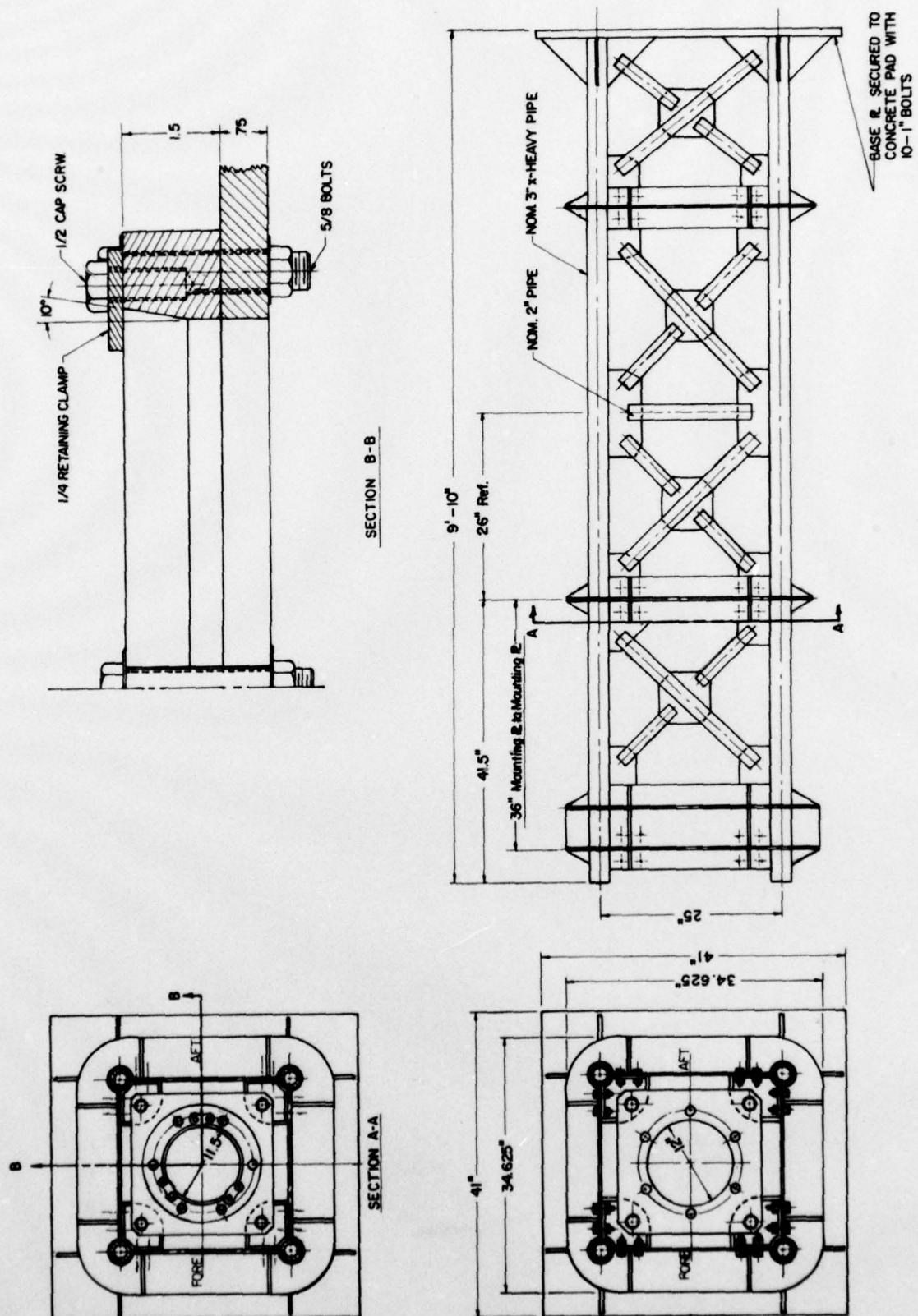
FIG. 2   SCHEMATIC OF THE LATTICE STRUCTURE MOUNTING FOR THE PROTOTYPE POLEMAST ANTENNA
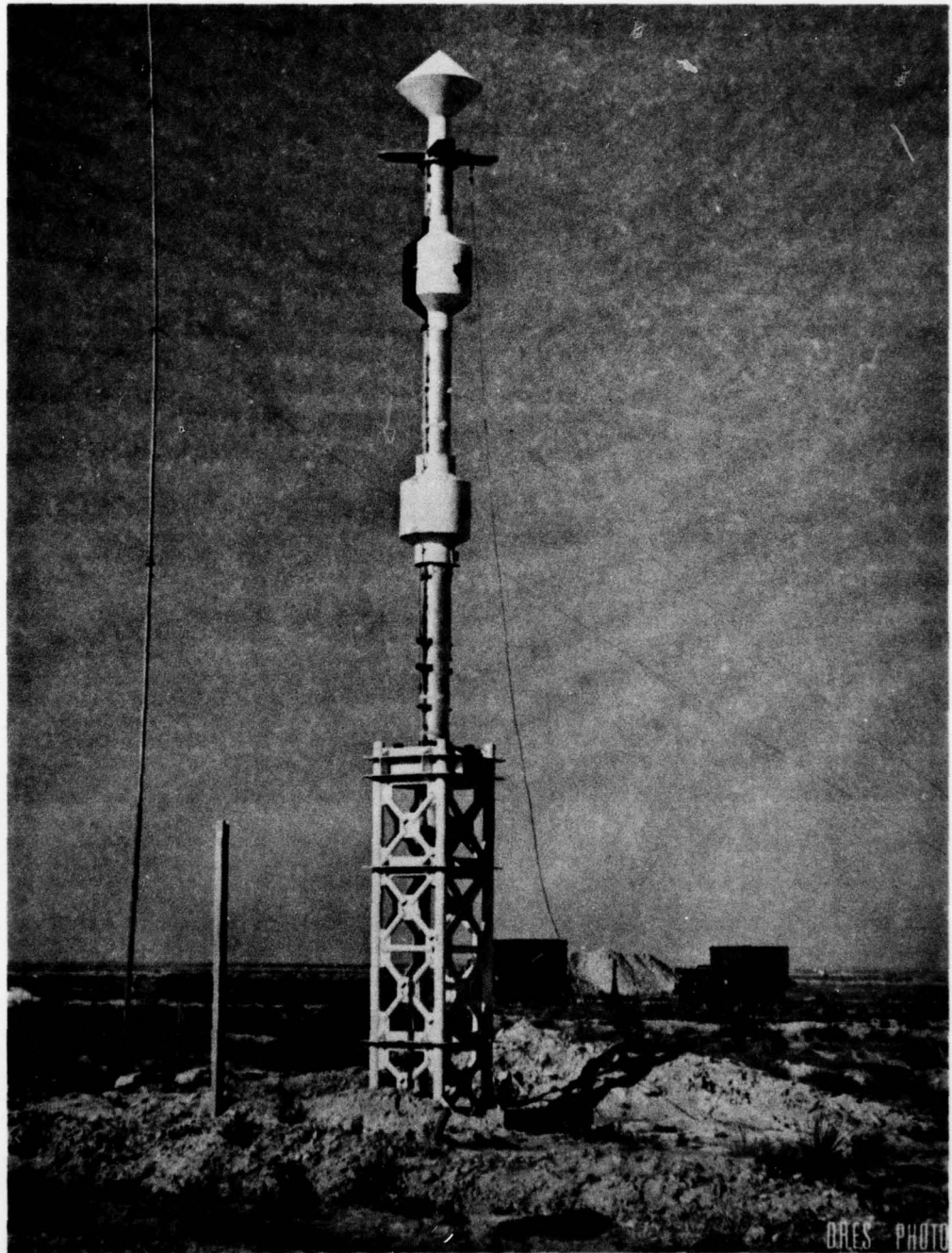
UNCLASSIFIED

FIG. 3   PHOTOGRAPH OF THE PROTOTYPE POLEMAST ANTENNA IN EVENT DICE THROW

ON-SITE INSTRUMENTATION

OFF-SITE DATA RECOVERY
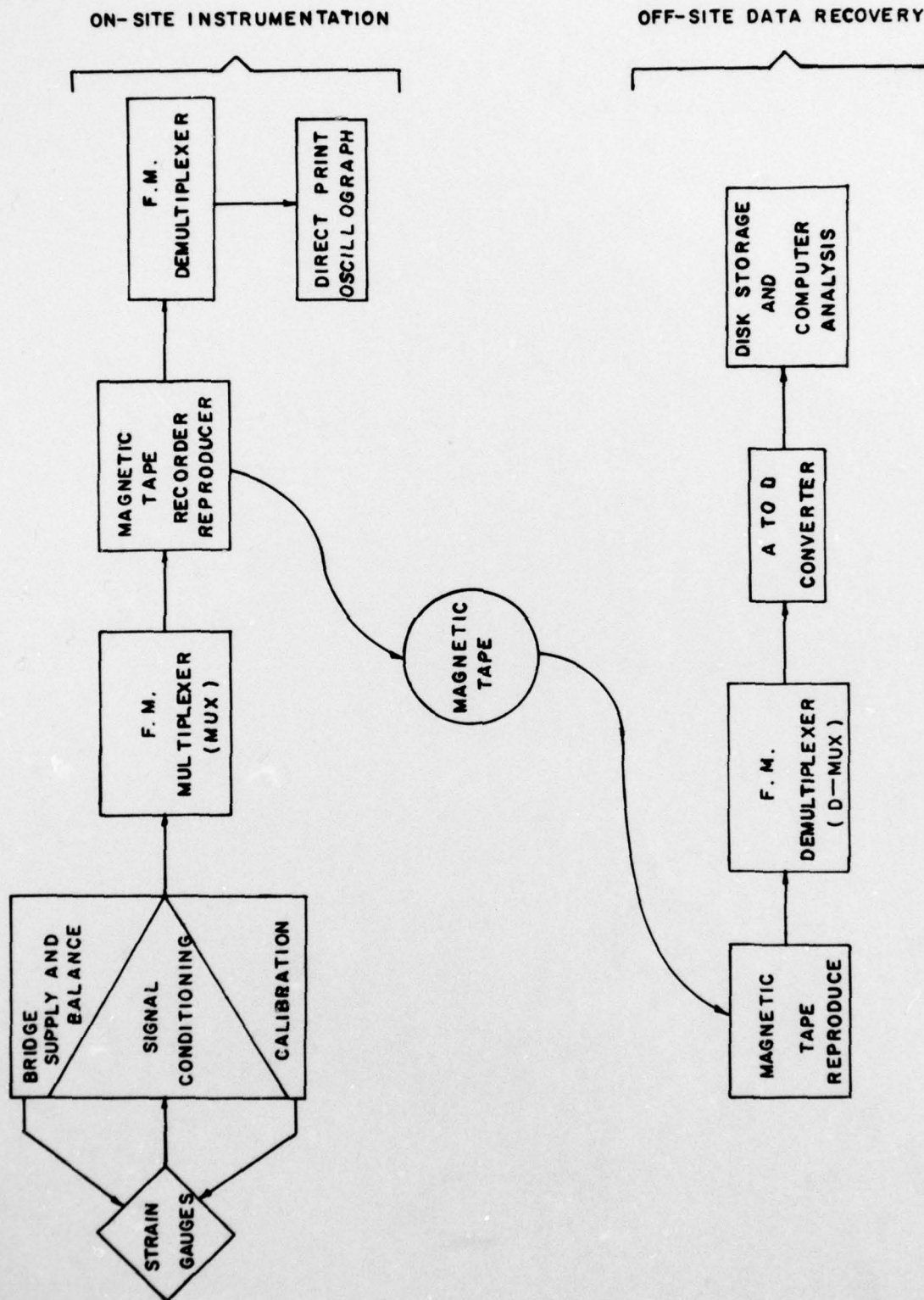
FIG. 4   SCHEMATIC DIAGRAM OF THE STRAIN GAUGE INSTRUMENTATION IN EVENT DICE THROW

FIG. 5 DRES INSTRUMENTATION BUNKER IN EVENT DICE THROW
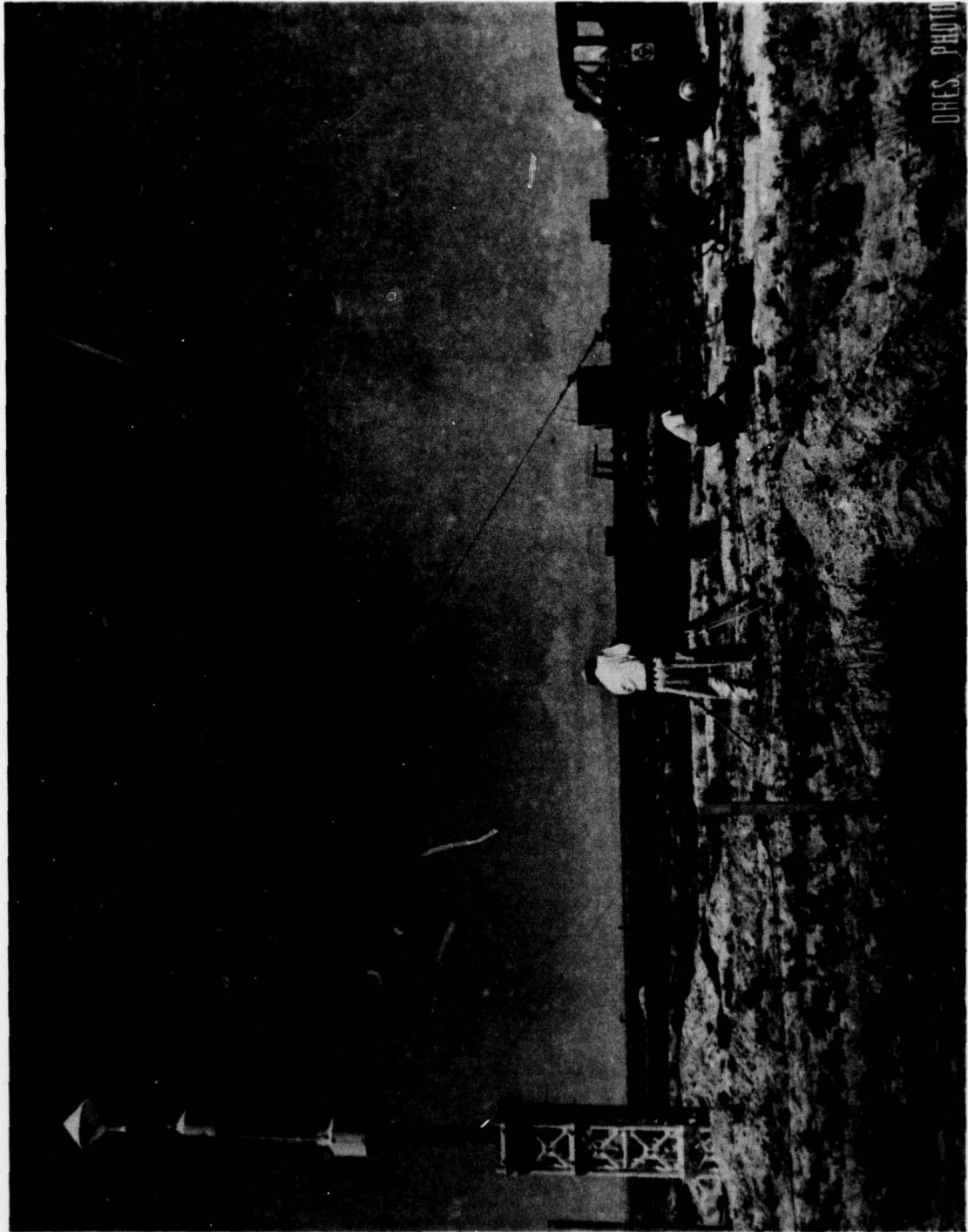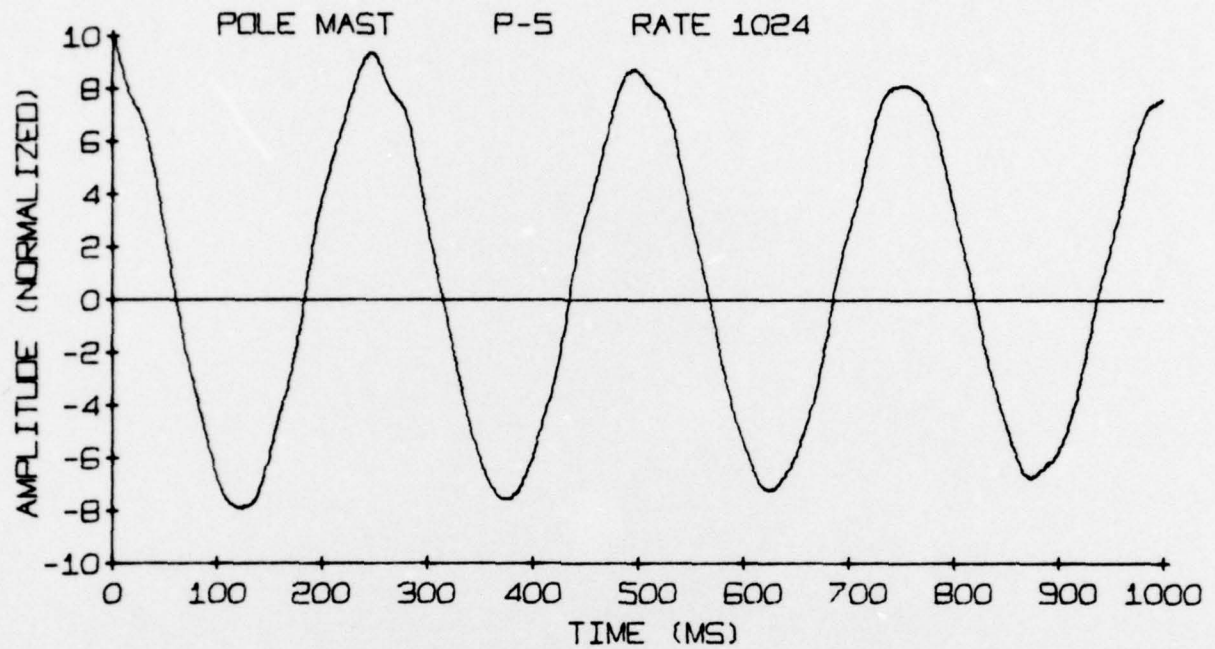
FIG. 6   PHOTOGRAPH OF THE TWANG TEST APPARATUS
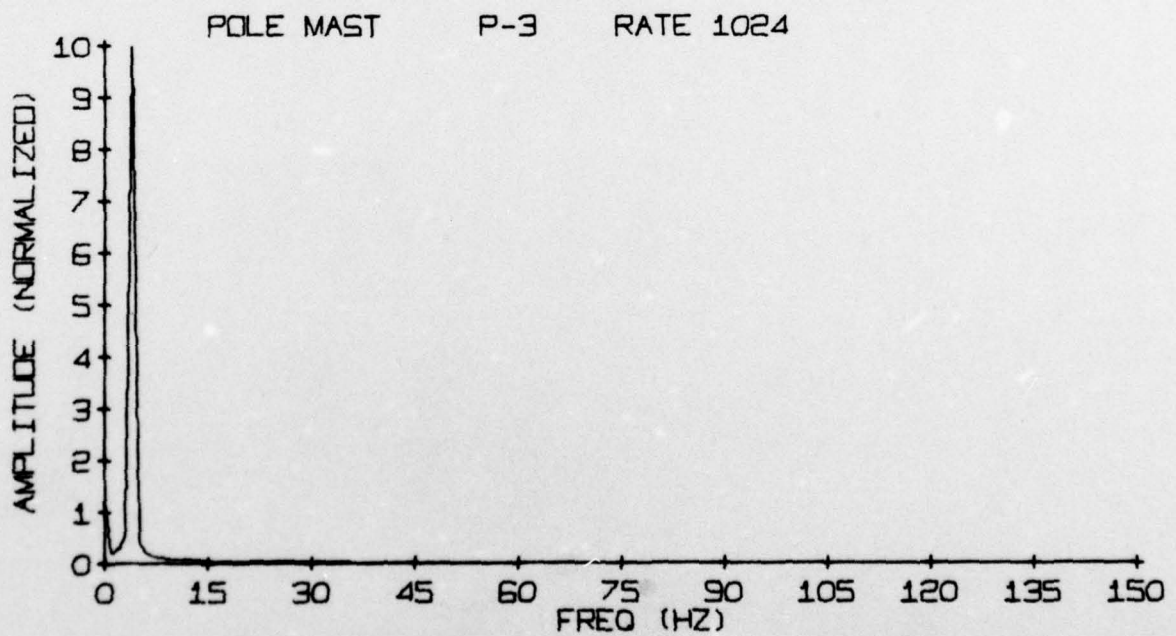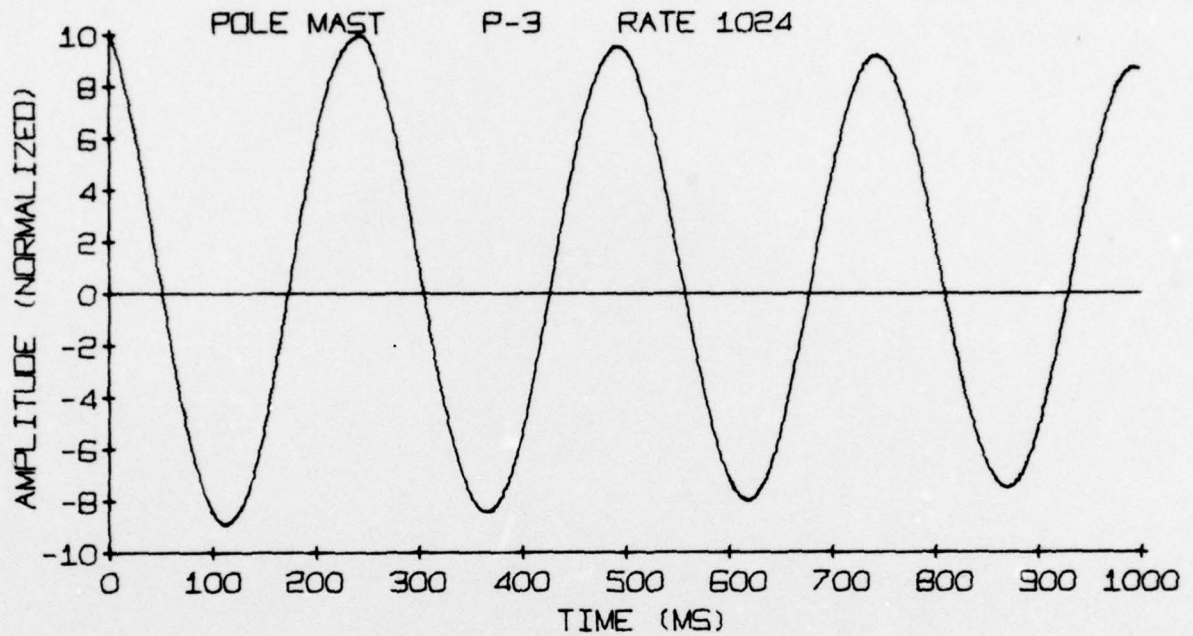
FIG. 7   TWANG TEST BENDING STRAIN HISTORY AND CORRESPONDING FOURIER
         ANALYSIS FOR GAUGE 3

UNCLASSIFIED

POLE MAST   P-5   RATE 1024

AMPLITUDE (NORMALIZED)

TIME (MS)

POLE MAST   P-5   RATE 1024

AMPLITUDE (NORMALIZED)

FREQ (HZ)
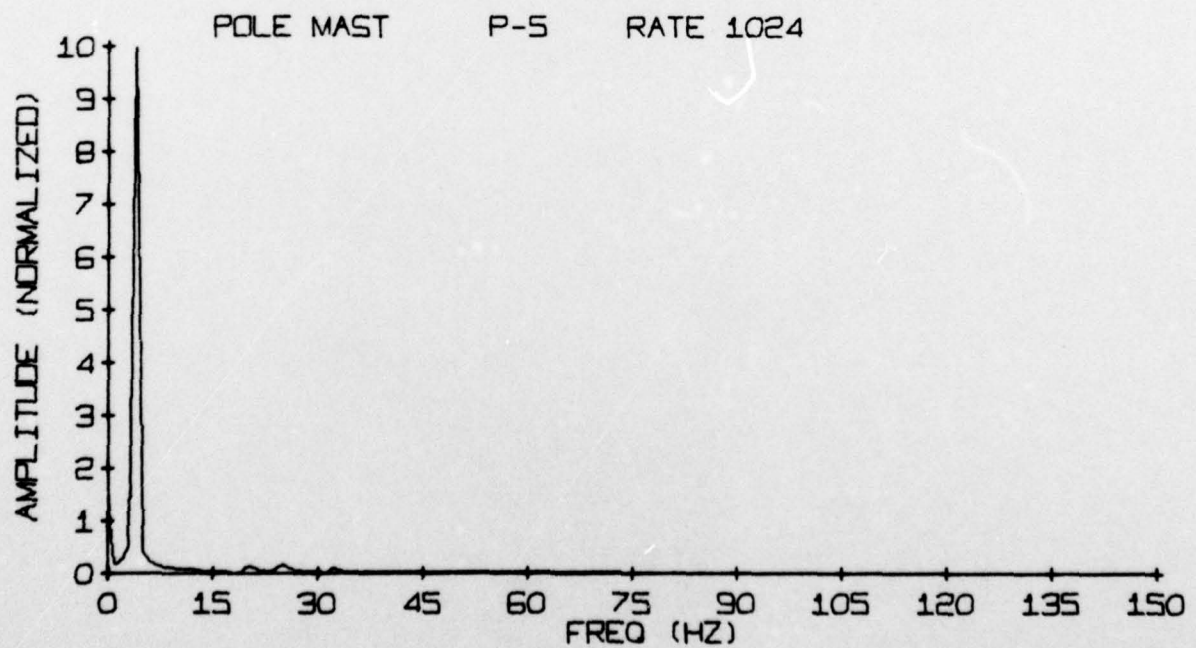
FIG. 8   TWANG TEST BENDING STRAIN HISTORY AND CORRESPONDING FOURIER
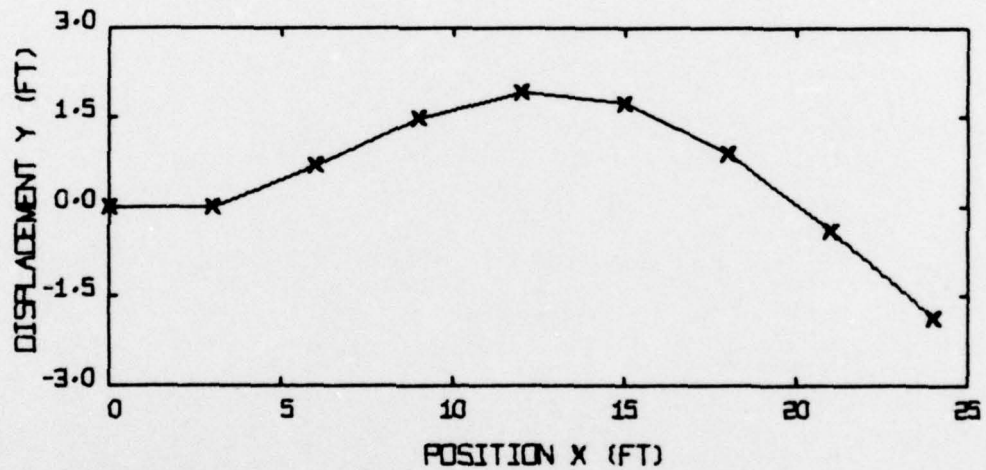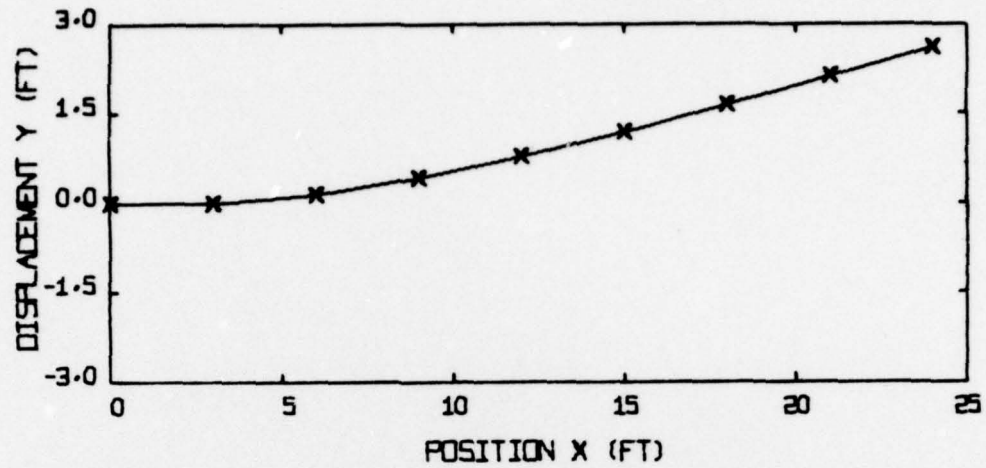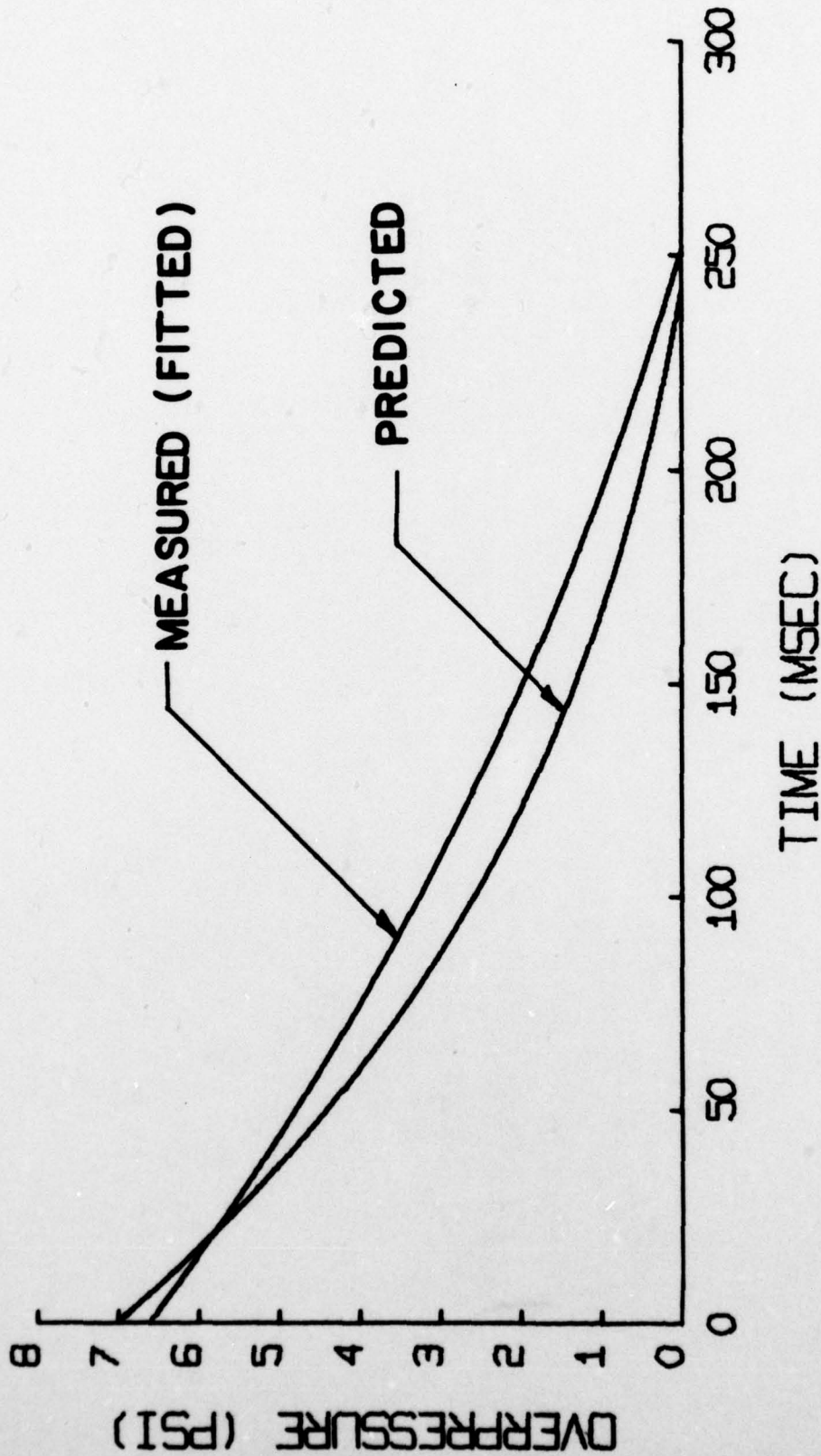ANALYSIS FOR GAUGE 5

UNCLASSIFIED
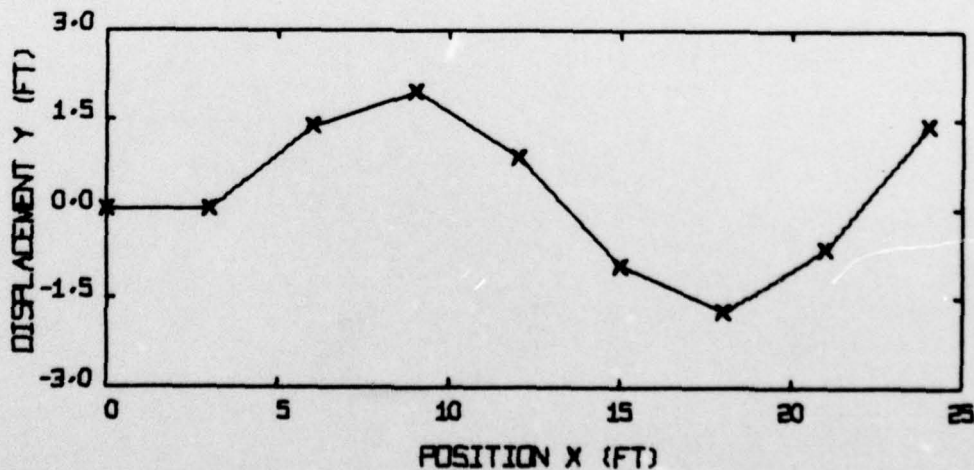
FIG. 9   THEORETICAL (NUMERICAL SIMULATION) PREDICTIONS FOR THE THREE
LOWEST NATURAL FREQUENCIES AND CORRESPONDING NORMAL MODES FOR
THE POLEMAST ANTENNA

FIG. 10   COMPARISON OF THE FRIEDLANDER WAVE WHICH CORRESPONDS TO THE PRE-TRIAL DNA
OVERPRESSURE PREDICTIONS AGAINST THE FRIEDLANDER WAVE WHICH CORRESPONDS TO
AVERAGE EXPERIMENTAL OVERPRESSURE MEASUREMENTS

NOMINAL VS. EXPERIMENTAL OVERPRESSURE
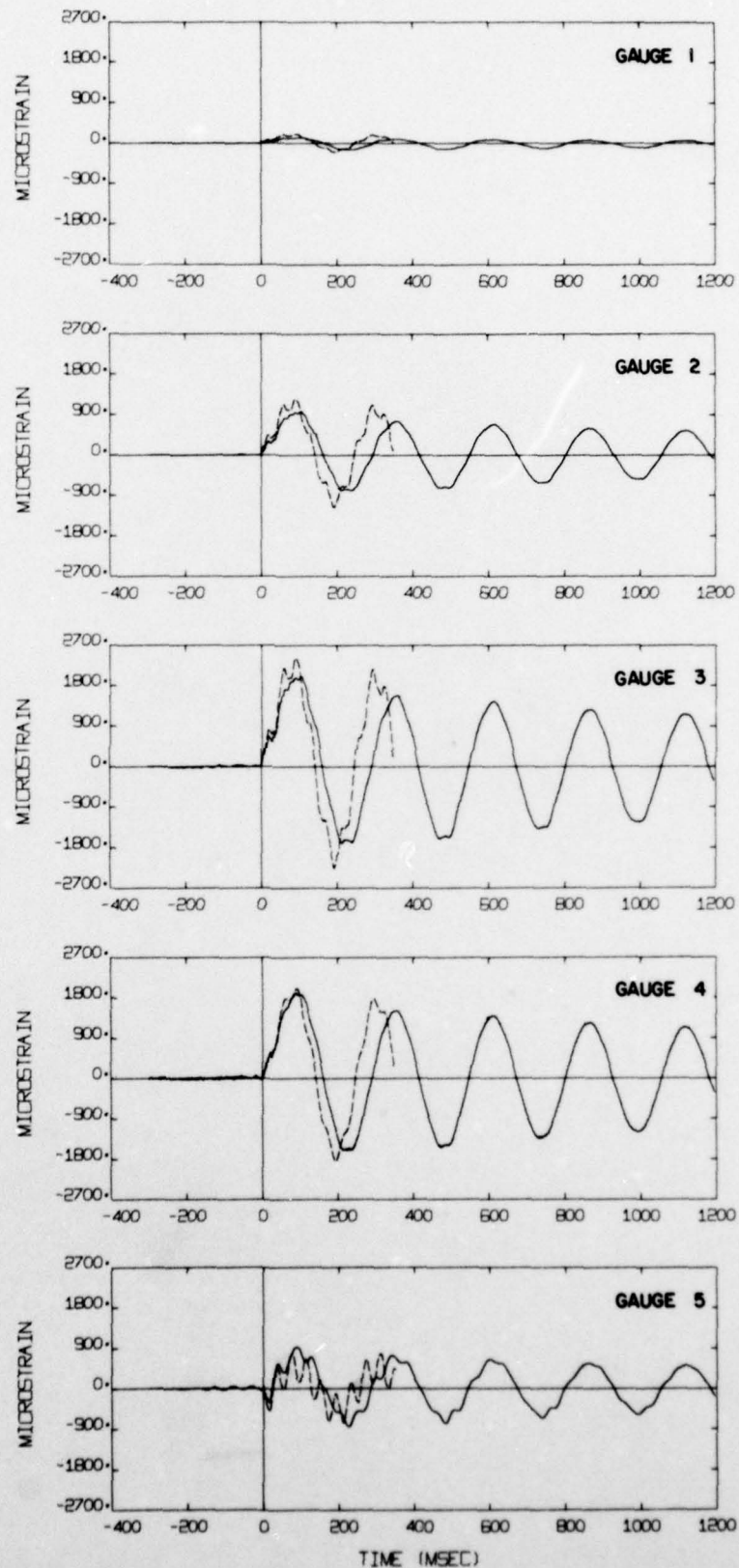
FIG. 11   COMPARISON OF BENDING STRAIN PREDICTIONS A (DASHED LINES)
          AGAINST THE MEASURED STRAINS (SOLID LINES) AT GAUGE LOCATIONS
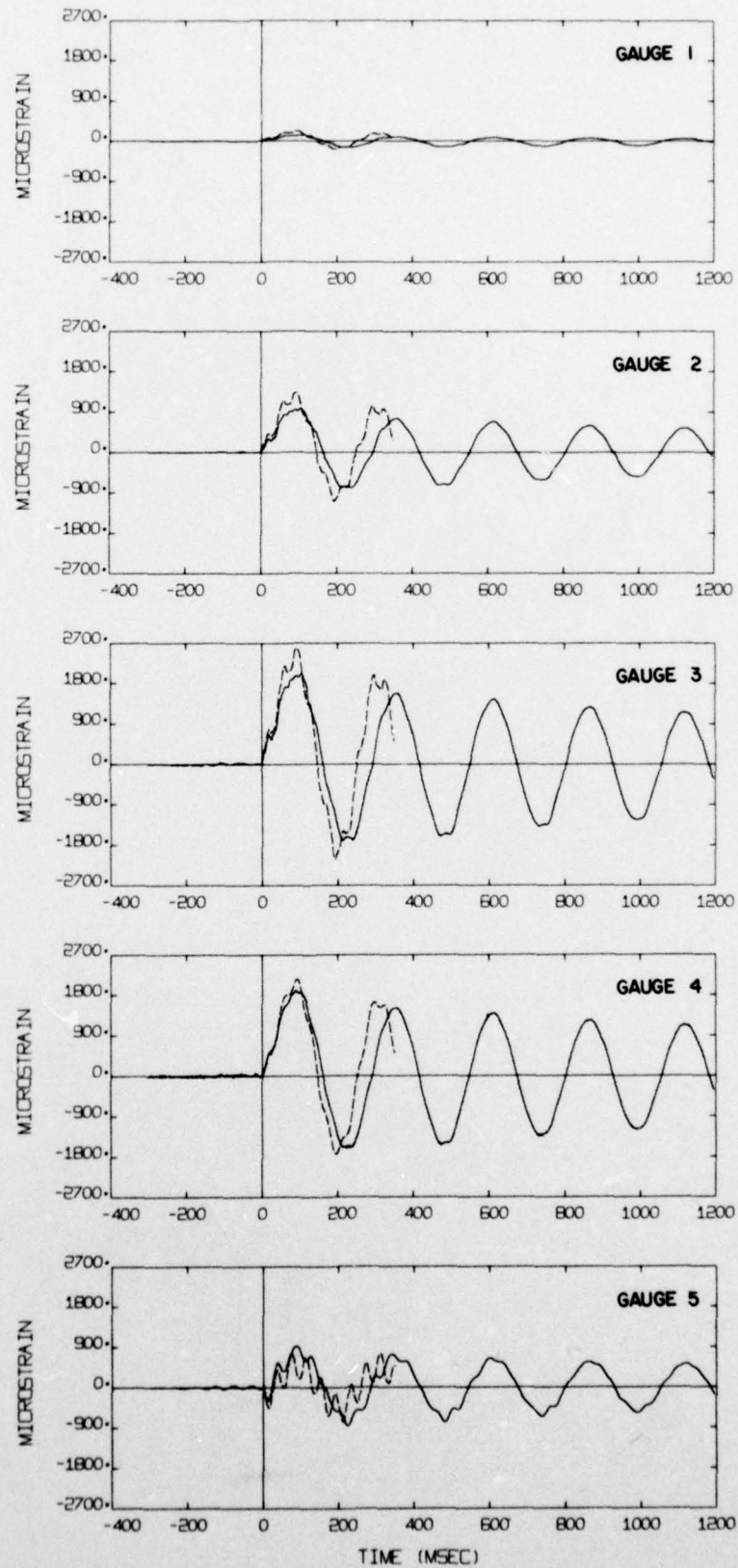   1 TO 5

FIG. 12   COMPARISON OF BENDING STRAIN PREDICTIONS B (DASHED LINES) AGAINST
THE MEASURED STRAINS (SOLID LINES) AT GAUGE LOCATIONS 1 TO 5

FIG. 13   COMPARISON OF BENDING STRAIN PREDICTIONS B(DASHED LINES) AGAINST THE MEASURED
STRAINS (SOLID LINES) AT GAUGE LOCATION 1

FIG. 14   COMPARISON OF BENDING STRAIN PREDICTIONS B (DASHED LINES) AGAINST THE MEASURED
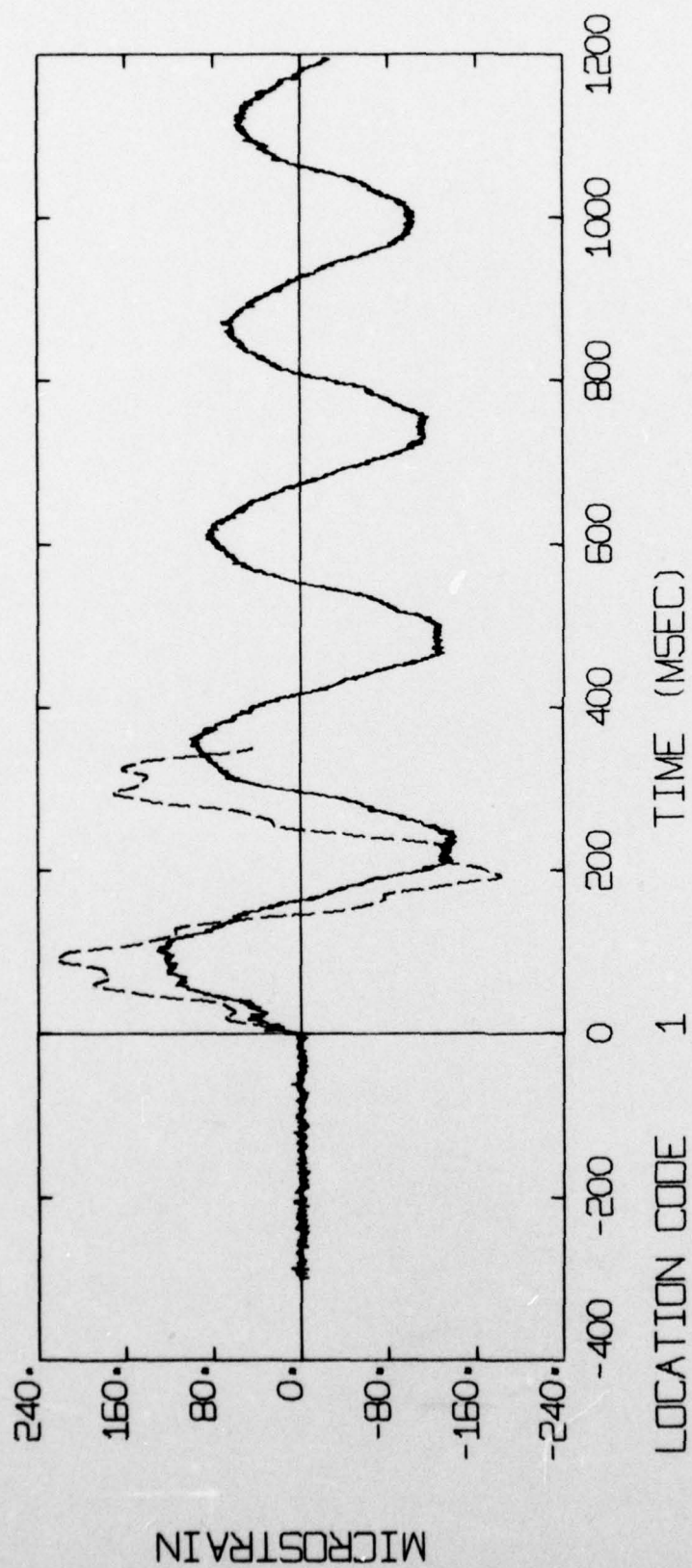STRAINS (SOLID LINES) AT GAUGE LOCATION 2

FIG. 15   COMPARISON OF BENDING STRAIN PREDICTIONS B (DASHED LINES) AGAINST THE MEASURED
STRAINS (SOLID LINES) AT GAUGE LOCATION 3

FIG. 16   COMPARISON OF BENDING STRAIN PREDICTIONS B (DASHED LINES) AGAINST THE MEASURED
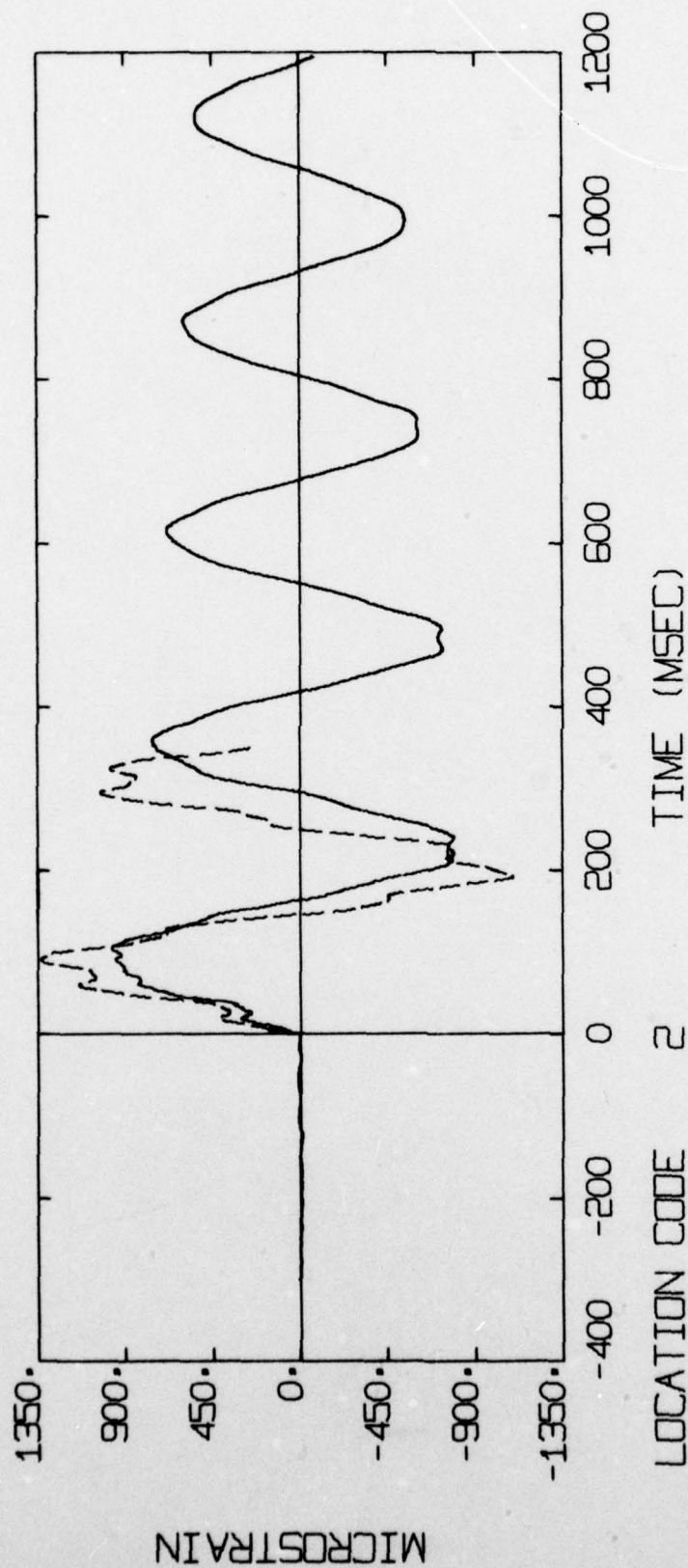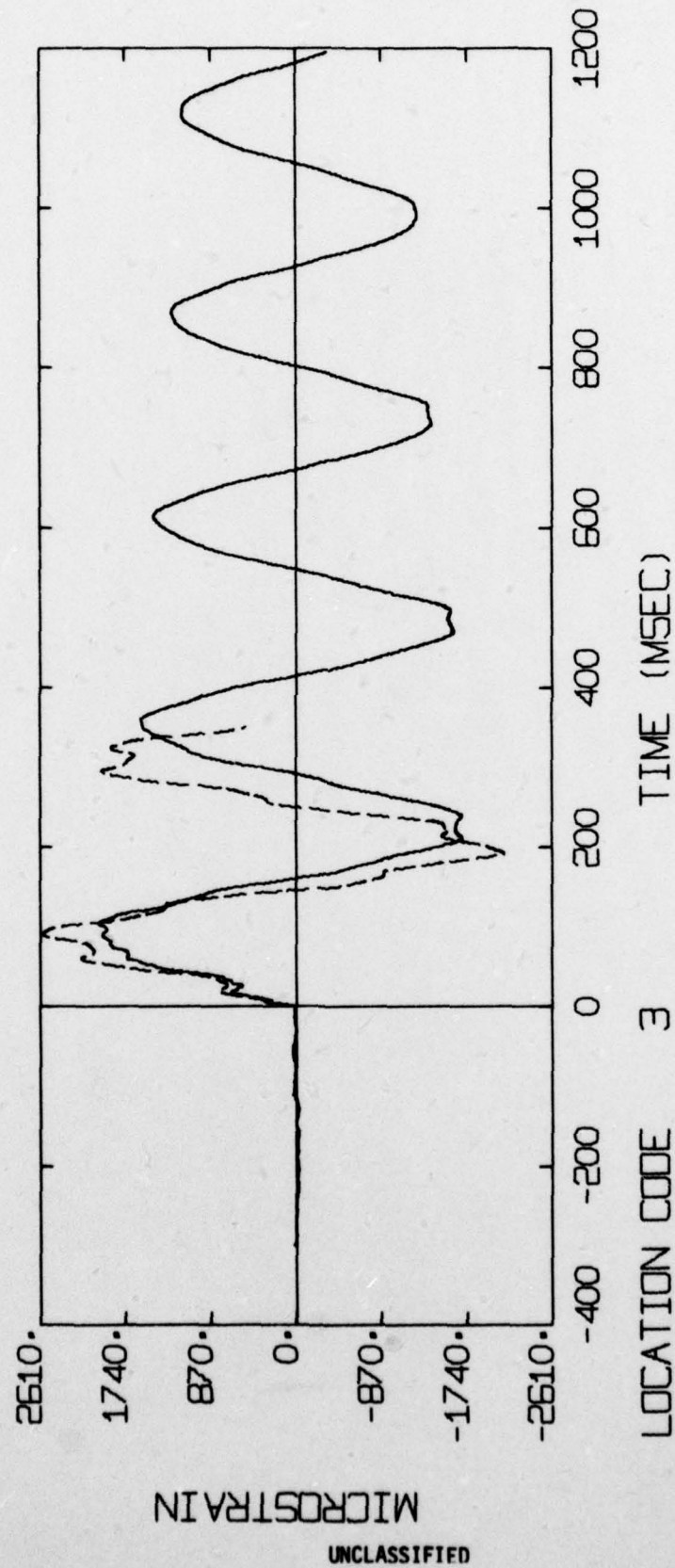   STRAINS (SOLID LINES) AT GAUGE LOCATION 4

FIG. 17 COMPARISON OF BENDING STRAIN PREDICTIONS B (DASHED LINES) AGAINST THE MEASURED STRAINS (SOLID LINES) AT GAUGE LOCATION 5

FIG. 18   COMPARISON OF BENDING STRAIN PREDICTIONS C (DASHED LINES) AGAINST
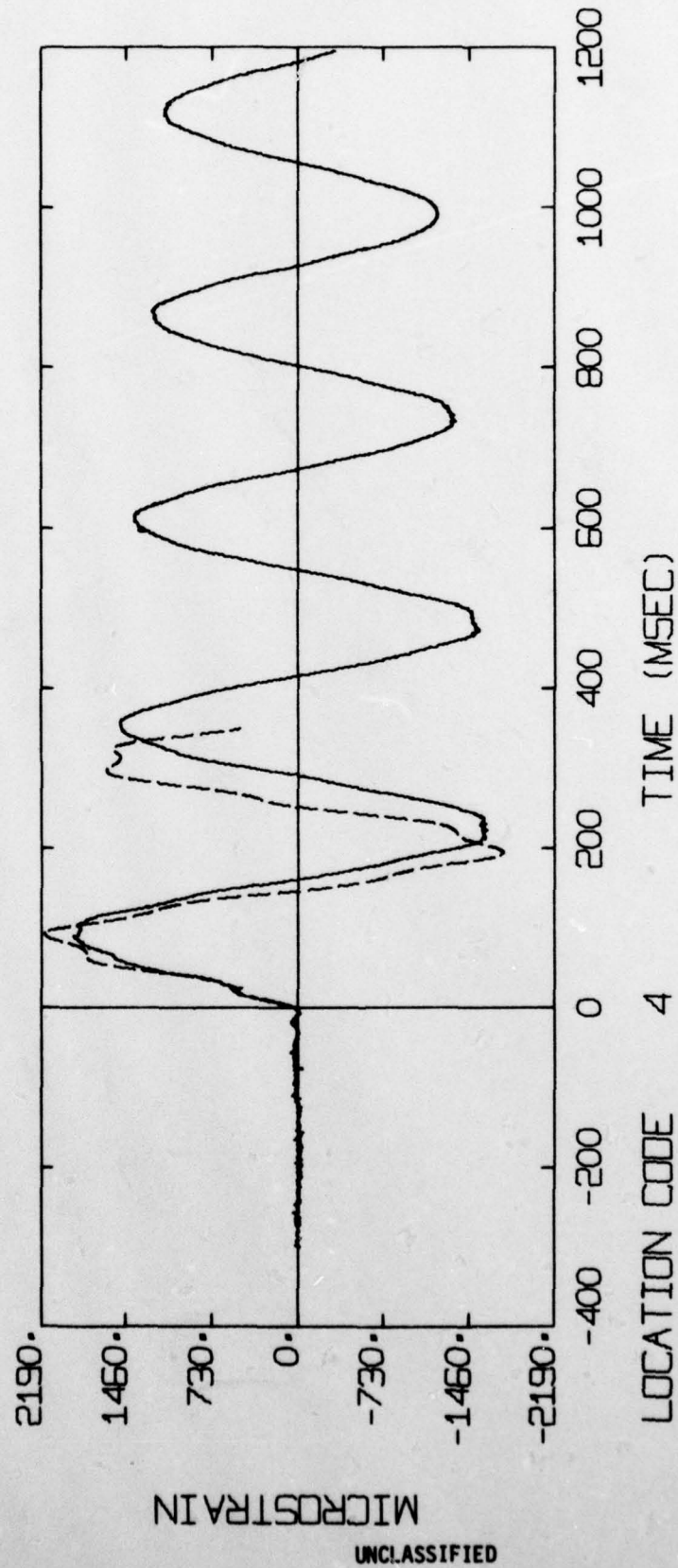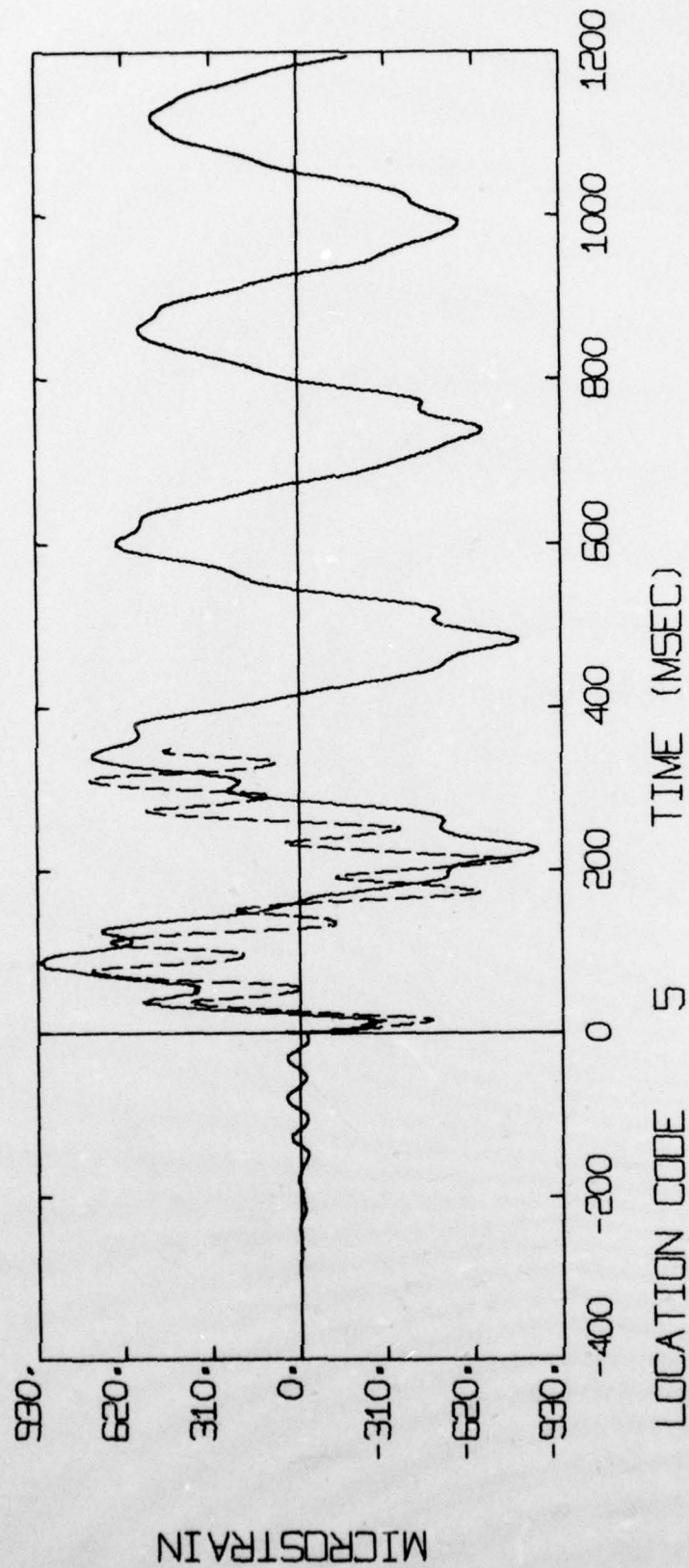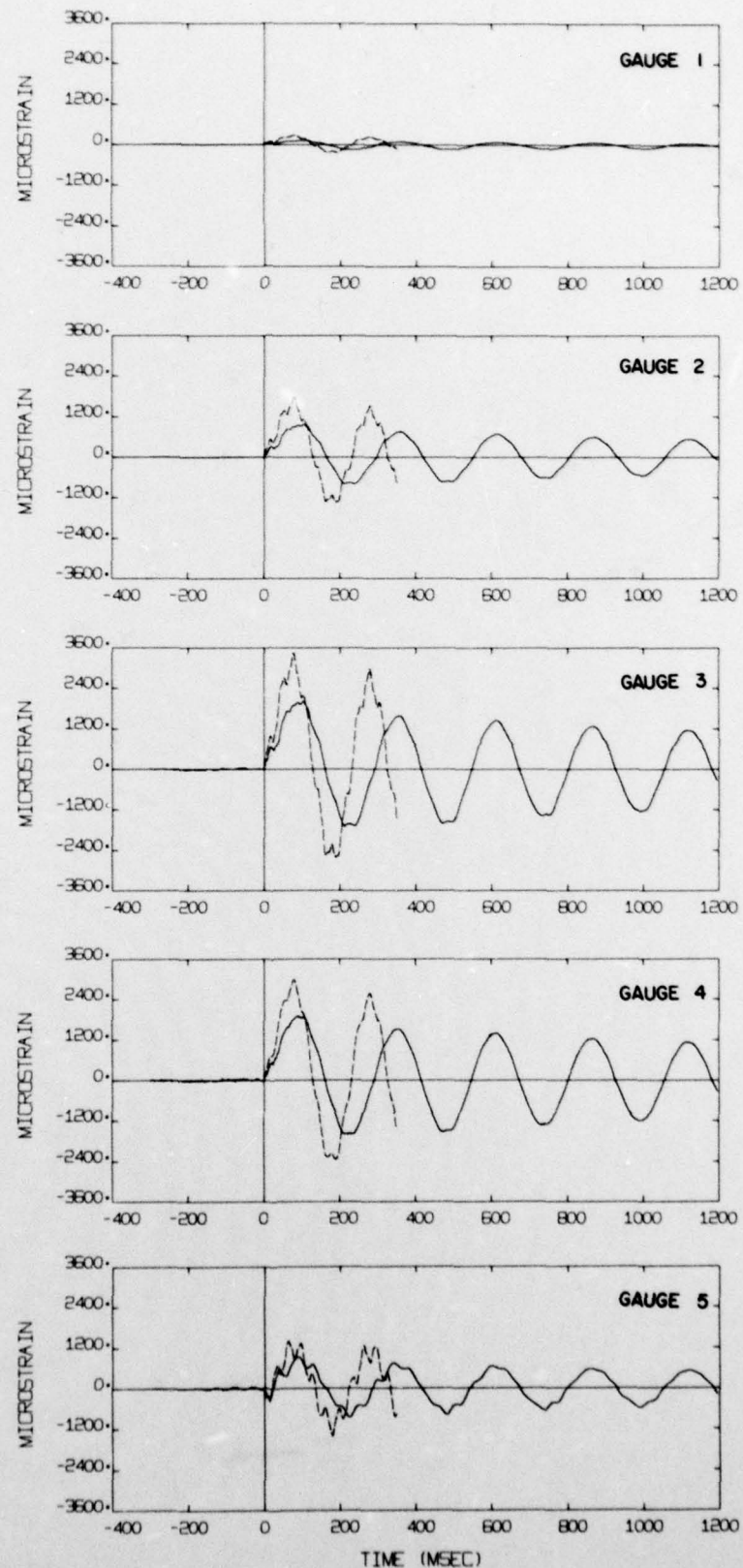THE MEASURED STRAINS (SOLID LINES) AT GAUGE LOCATIONS 1 TO 5
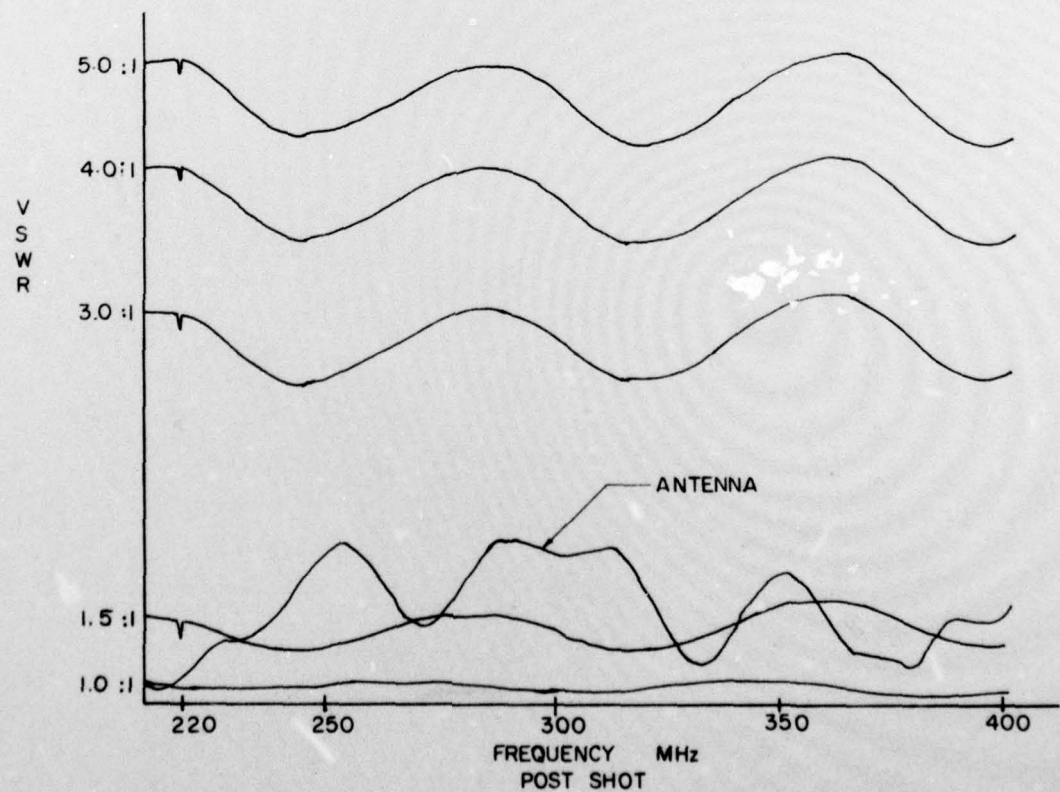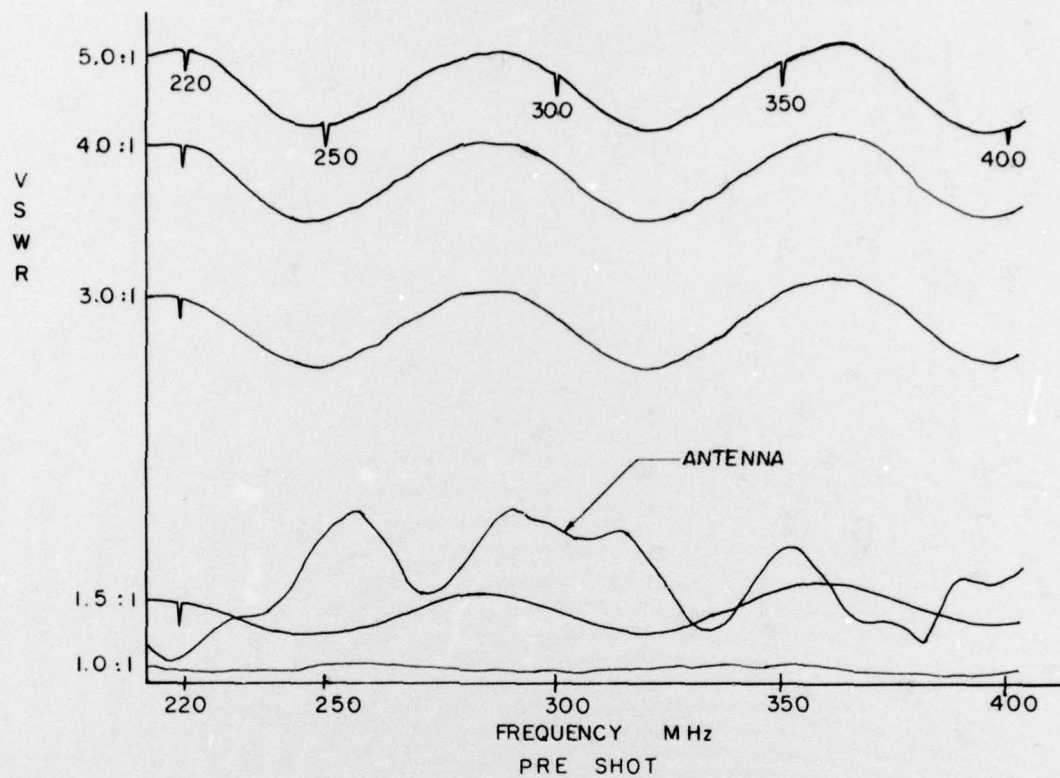
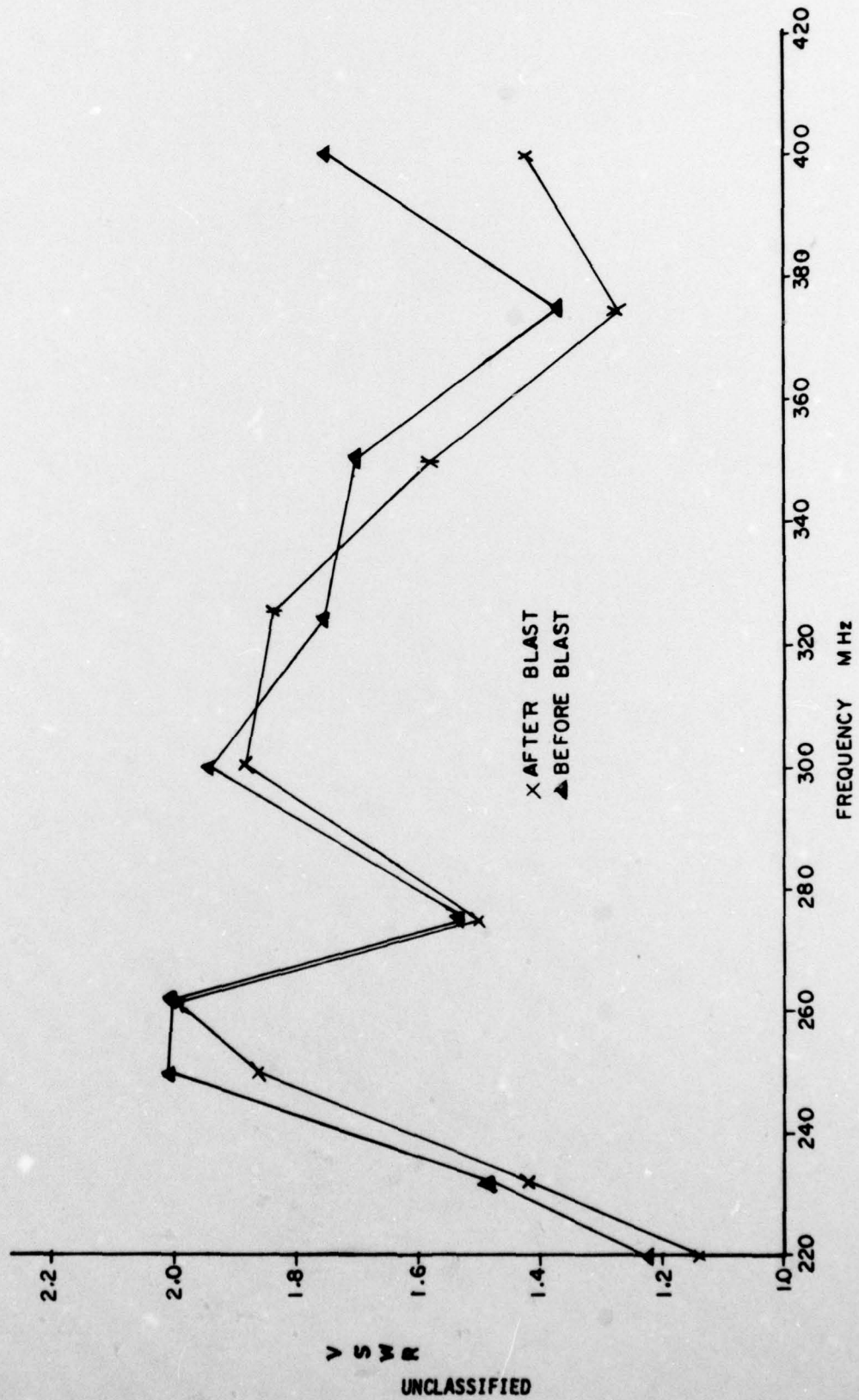FIG. 19   PRE-TRIAL AND POST-TRIAL VSWR TEST RESULTS

FIG. 20   PRE-TRIAL AND POST-TRIAL CALCULATED VALUES OF THE VSWR VERSUS FREQUENCY

UNCLASSIFIED

DEFENCE RESEARCH ESTABLISHMENT SUFFIELD
RALSTON ALBERTA

APPENDIX A

PROTOTYPE UHF POLEMAST ANTENNA DESIGN MODIFICATIONS

During the fabrication of the prototype Polemast at DRES,
design modifications were required in order to accommodate the facilities
of the Machine Shop (the DRES Machine Shop is considered to be well
equipped). It is anticipated that the suggested design changes will
generally make the item more cost effective and open to a greater number
of fabricators during the tendering for the lot production.

The design modifications are summarized below in tabular form.
A justification for the individual modifications is considered immediately
following the table.

Description	Drawing No.	Modification
(a) Top Inside Flange Ring	DDDS-000147	• see Figure A-1
(b) Polemast Weldment Assembly	DDDS-000159	• material change
		• delete machining on the OD and ID of the mast
(c) Screen	DDD-000145	• delete welding and assemble by riveting
		• replace round bar stock with square
(d) Clamp Assembly	DDD-000143	• see the footnote
(e) Tolerance	—	• see the footnote

TABLE A-1: UHF Polemast Antenna design modifications.

(a) Welding the bottom face of the flange as shown in the drawing
to the inside diameter of the tube was not possible. In addition, to ensure
a flat surface without machining the top face of the flange, it was necessary
to design a mounting as shown in Figure A-1.

UNCLASSIFIED

(b) The original material specification was 6061-T6 aluminum with a 1/4 in wall and a 9-1/2 in outside diameter (OD). Based on the recommendation of an Alcan representative and a preliminary stress analysis (7), the material was changed to 6351-T6 aluminum. A 9-1/2 in OD by 1/4 in wall extrusion was not available in Canada. The closest acceptable substitute was a 9-1/2 in OD by 0.261 in wall extrusion die.

Machining, as specified on the drawing, was deleted since a lathe of sufficient size was not available. This should be considered a permanent modification since the dimensions of the top clamp can accommodate the tolerance of seamless extruded tubing as specified by the Aluminum Association, and the bottom and top rings can be machined to suit the tube.

It should be noted that tube ovality was removed both when determining the diameter by the use of "C" clamps and when fitting the bottom ring to the tube. Heat distortion in welding the ring to the tube produced a 0.020 in ovality in the ring. This did not cause a problem with assembly. Complete circumferential seating was achieved when the Polemast was mounted into the lower clamp.

(c) Welding, as specified in the drawing, was unacceptable due to heat distortion. Substituting a heavier gauge material did not resolve the welding heat distortion problem. Following are the design modifications which resolved the problem: (i)   replace 20 gauge material with 14 gauge; (ii) replace round stock with 1/4 in square stock (cold rolled steel was used in place of 6061-T6 AL as the AL was not available in time for the trial); and (iii) welding was replaced with riveting, using 1/8 in diameter by 7/16 in long 16 ST AL rivets on a 1/2 in pitch. All surfaces were zinc chromated before assembly.

(d) Clamp Assembly was fabricated according to the drawing. However, due to the large heat distortion caused by welding (approximately 1/16 in on the 9-1/2 in diameter and 3/32 in curvature on the flange), the following design modifications are recommended: 3/8 in thick material should be used for the collar, and 3/4 in plate should be used for the flange (machined perpendicular to the 9-1/2 in diameter after welding).

(e) Based on modification (b) described above, items such as the Clamp Assembly, Top Inside Flange Ring, and Bottom Ring could have looser tolerances to accommodate the tube as supplied. The following information was determined for a random sample of aluminum tubes taken from the 25 20-ft (nominal) lengths (measurements at 32°F): minimum OD - 9.507 in, maximum OD - 9.548 in, minimum wall thickness - 0.248 in, maximum wall thickness OD - 0.271 in. It is noted that the above dimensions are well within the allowable specifications for seamless extruded tubing, as specified by the Aluminum Association.
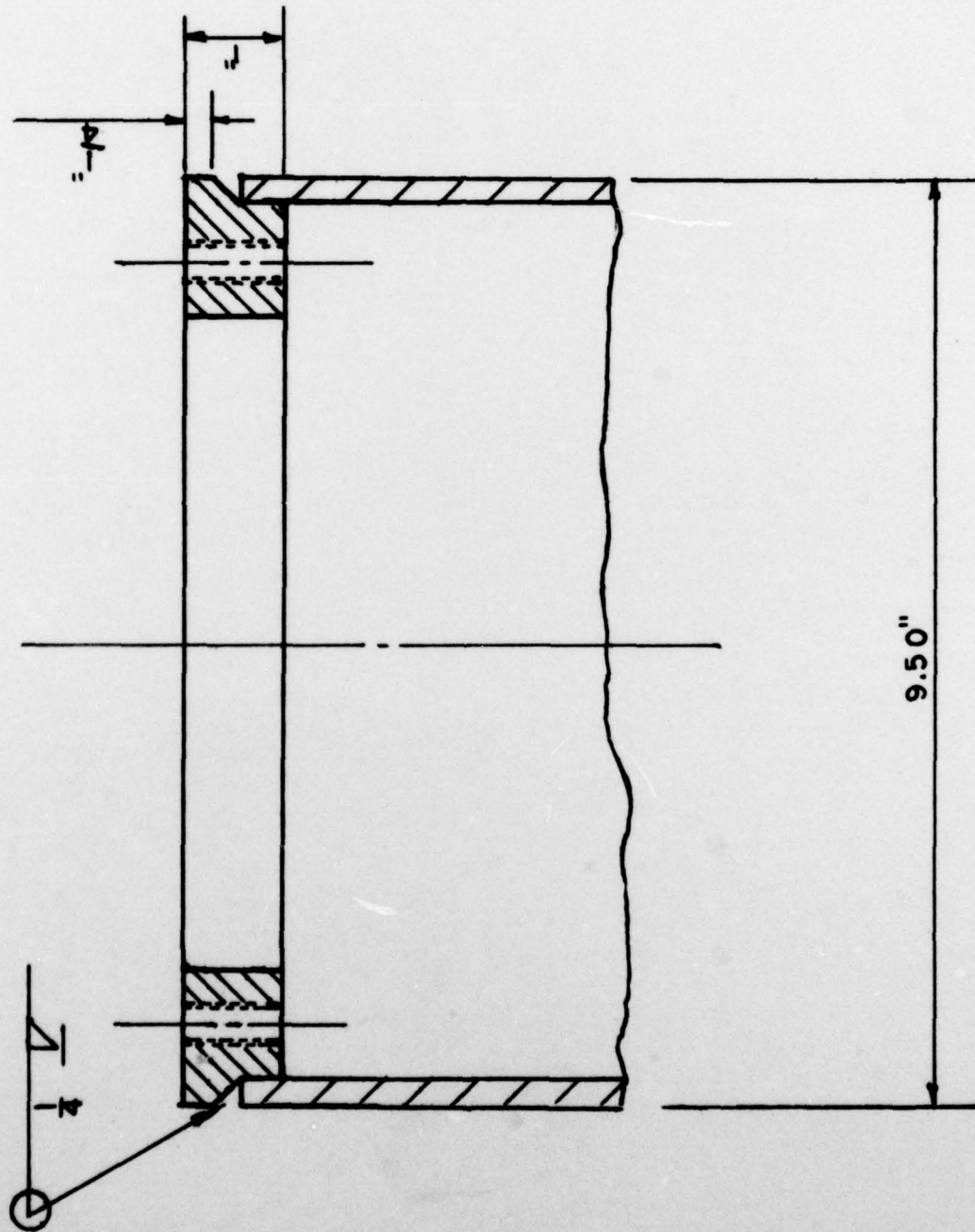
9.50"

FIG. A1   MODIFIED TOP INSIDE FLANGE RING USED ON THE PROTOTYPE UHF POLEMAST ANTENNA

DEFENCE RESEARCH ESTABLISHMENT SUFFIELD
RALSTON ALBERTA

APPENDIX B

PHYSICAL PROPERTIES OF THE POLEMAST ANTENNA ALUMINUM TUBING

The structural portion of the prototype Polemast Antenna is a seamless aluminum tube of length 19 ft 7.5 in. This tubing was fabricated by Alcan Canada Products Ltd. according to Department of Supply and Services Contract No. CAL75-5942/1 (8). Following is a summary of the physical and chemical properties of the aluminum tubing, as provided by an Alcan "Release Note and Certificate" (9):

Material: 6351-T6 aluminum extruded seamless tubing with a 0.261 in
         wall and 9.5 in outside diameter, supplied in nominal 20-ft
         lengths. Total weight of the 25 pieces supplied was 4430 lb.

Alcan Order Number: 11-76-02595.

Consignee: Wilkinson Co. Ltd., Calgary, Alberta.

Identification: 12-47-209.

Tensile Strength (psi): 49,300.

Yield Stress (psi): 45,000 (0.2% offset).

Elongation (%):   14.

Gauge (in):   2.

Chemical Compositions Limits (% weight):

	Al	Cu	Fe	Mg	Mn	Ni	Si	Ti	Zn	Cr	Zr	Other Each	Total	Fe+Si
Max.		.10	.50	.8	.8		1.3	.20	.20			.05		.15
Min.				.40	.40		.7							

In order to obtain confirmation of the tensile properties of the aluminum tubing in the prototype Polemast, four test specimens were machined from the 4.5 in surplus piece which was removed to bring the tube to its design length. The specimens were fabricated according to

ASTM standard A370-71 for round tension test specimens. The tests were performed and certified by R.M. Hardy and Associates Ltd., Metallurgical Division, Calgary. Tensile properties of the specimens are outlined below in tabular form (10). It may be concluded from this table that the aluminum tubing meets or exceeds the manufacturer's specifications for tensile properties of 6351-T6 aluminum.

Specimen deminsions:

Specimens were cut parallel to the longitudinal axis of the tube.
Gauge length: 0.750 in
Gauge diameter: 0.160 in
Specimen overall length: 4.5 in
Grip section diameter: .25 in
Grip section thread: 20 threads/in

Stress	Specimen Number				
(psi)	1	2	3	4	Average
Ultimate	51,650	51,083	51,243	50,845	51,205
Yield [1]	48,058	46,851	47,263	47,263	47,358

[1] 0.2% offset

TABLE B1:   Tensile tests on 6451-T6 aluminum tubing.

UNCLASSIFIED

REFERENCES

1. G.V. Price, "Numerical Simulation of The Air Blast Response of Tapered Cantilever Beams", Defence Research Establishment Suffield, Ralston, Alberta. Suffield Technical Paper No. 447. 1977. UNCLASSIFIED.

2. C.G. Coffey, "Blast Response of the GRP Topmast (U)". Suffield Memorandum No. 10/71. .1971. UNCLASSIFIED.

3. R. Naylor and S.B. Mellsen, "Unsteady Drag From Free-Field Blast Waves (U)". Defence Research Establishment Suffield, Ralston, Alberta. Suffield Memorandum No. 42/71. 1973. UNCLASSIFIED.

4. B.R. Long, B.G. Laidlaw and R.J. Smith, "The Analysis of Shipboard Lattice Antenna Masts Under Air Blast and Underwater Shock Loading, Part III - Final Report (U)". Defence Research Establishment Suffield, Ralston, Alberta. Suffield Technical Paper No. 431. 37 pp. 1975. UNCLASSIFIED.

5. F.H. Winfield, "Event Dice Throw - Canadian Air Blast Measurements (U)". Suffield Technical Paper No. 451. 1977. UNCLASSIFIED.

6. C.G. McIntyre, Trip Report of P. Sparrow, Private Communication to C.G. Coffey. File No. 10011-3656356 (DMCS-6). Received 2 November 1976.

7. C.G. Coffey, Private communication to R. McInnis , NDHQ/DMCS-6. DRES File No. 3611F-8. 18 June 1976.

8. Department of Supply and Services Contract No. CAL75-5942/1. 13 April 1976.

9. Alcan Products Ltd. Release Note and Certificate to Wilkinson Co. Ltd. Calgary. 6 August 1976.

10. R.M. Hardy and Associates Metal Test Report L76-1645. Private Communication to G.V. Price. 25 August 1976.

UNCLASSIFIED

UNCLASSIFIED
Security Classification

DOCUMENT CONTROL DATA - R & D

(Security classification of title, body of abstract and indexing annotation must be entered when the overall document is classified)

1. ORIGINATING ACTIVITY	2a. DOCUMENT SECURITY CLASSIFICATION
DEFENCE RESEARCH ESTABLISHMENT SUFFIELD	UNCLASSIFIED
	2b. GROUP

3. DOCUMENT TITLE

BLAST RESPONSE OF UHF POLEMAST ANTENNA - EVENT DICE THROW

4. DESCRIPTIVE NOTES (Type of report and inclusive dates)

TECHNICAL PAPER

5. AUTHOR(S) (Last name, first name, middle initial)

Coffey, C.G. and Price, G.V. (10)   C.G. /Coffey G.V. /Price

6. DOCUMENT DATE	7a. TOTAL NO. OF PAGES	7b. NO. OF REFS
(11) Nov 77	47	10

8a. PROJECT OR GRANT NO.	9a. ORIGINATOR'S DOCUMENT NUMBER(S)
97-80-01	SUFFIELD TECHNICAL PAPER NO. 449
8b. CONTRACT NO.	9b. OTHER DOCUMENT NO.(S) (Any other numbers that may be assigned this document)

10. DISTRIBUTION STATEMENT	
UNLIMITED DISTRIBUTION	(12) 52 p.

11. SUPPLEMENTARY NOTES	12. SPONSORING ACTIVITY

13. ABSTRACT

The blast response of a 23 ft UHF Polemast Antenna was investigated in a free-field blast trial and in numerical simulation experiments. The antenna satisfactorily withstood the air blast loading at the nominal 7.0 psi peak overpressure location in Event Dice Throw, and the numerical model predictions for the natural frequencies and transient strain were in excellent agreement with the values obtained experimentally.

403 104

KEY WORDS

Dice Throw

Air Blast

Polemast Antenna

Navy

Transient Strain

Numerical Simulation

INSTRUCTIONS

1. **ORIGINATING ACTIVITY:** Enter the name and address of the organization issuing the document.

2a. **DOCUMENT SECURITY CLASSIFICATION:** Enter the overall security classification of the document including special warning terms whenever applicable.

2b. **GROUP:** Enter security reclassification group number. The three groups are defined in Appendix 'M' of the DRB Security Regulations.

3. **DOCUMENT TITLE:** Enter the complete document title in all capital letters. Titles in all cases should be unclassified. If a sufficiently descriptive title cannot be selected without classification, show title classification with the usual one-capital-letter abbreviation in parentheses immediately following the title.

4. **DESCRIPTIVE NOTES:** Enter the category of document, e.g. technical report, technical note or technical letter. If appropriate, enter the type of document, e.g. interim, progress, summary, annual or final. Give the inclusive dates when a specific reporting period is covered.

5. **AUTHOR(S):** Enter the name(s) of author(s) as shown on or in the document. Enter last name, first name, middle initial. If military, show rank. The name of the principal author is an absolute minimum requirement.

6. **DOCUMENT DATE:** Enter the date (month, year) of Establishment approval for publication of the document.

7a. **TOTAL NUMBER OF PAGES:** The total page count should follow normal pagination procedures, i.e., enter the number of pages containing information.

7b. **NUMBER OF REFERENCES:** Enter the total number of references cited in the document.

8a. **PROJECT OR GRANT NUMBER:** If appropriate, enter the applicable research and development project or grant number under which the document was written.

8b. **CONTRACT NUMBER:** If appropriate, enter the applicable number under which the document was written.

9a. **ORIGINATOR'S DOCUMENT NUMBER(S):** Enter the official document number by which the document will be identified and controlled by the originating activity. This number must be unique to this document.

9b. **OTHER DOCUMENT NUMBER(S):** If the document has been assigned any other document numbers (either by the originator or by the sponsor), also enter this number(s)

10. **DISTRIBUTION STATEMENT:** Enter any limitations on further dissemination of the document, other than those imposed by security classification, using standard statements such as:

　(1)　"Qualified requesters may obtain copies of this document from their defence documentation center."

　(2)　"Announcement and dissemination of this document is not authorized without prior approval from originating activity."

11. **SUPPLEMENTARY NOTES:** Use for additional explanatory notes.

12. **SPONSORING ACTIVITY:** Enter the name of the departmental project office or laboratory sponsoring the research and development. Include address.

13. **ABSTRACT:** Enter an abstract giving a brief and factual summary of the document, even though it may also appear elsewhere in the body of the document itself. It is highly desirable that the abstract of classified documents be unclassified. Each paragraph of the abstract shall end with an indication of the security classification of the information in the paragraph (unless the document itself is unclassified) represented as (TS), (S), (C), (R), or (U).

The length of the abstract should be limited to 20 single-spaced standard typewritten lines; 7½ inches long.

14. **KEY WORDS:** Key words are technically meaningful terms or short phrases that characterize a document and could be helpful in cataloging the document. Key words should be selected so that no security classification is required. Identifiers, such as equipment model designation, trade name, military project code name, geographic location, may be used as key words but will be followed by an indication of technical context.